THE JOURNAL OF BIOLOGICAL CHEMISTRY
Vol. 276, No. 26, Issue of June 29, pp. 23329–23340, 2001

Printed in U.S.A.

Cyclosporin A Inhibits Inositol 1,4,5-Trisphosphate-dependent Ca^{2+} Signals by Enhancing Ca^{2+} Uptake into the Endoplasmic Reticulum and Mitochondria*

Received for publication, February 1, 2001, and in revised form, April 11, 2001
Published, JBC Papers in Press, April 25, 2001, DOI 10.1074/jbc.M100989200

Soraya S. Smaili‡, Kerri Anne Stellato§, Paul Burnett§, Andrew P. Thomas§, and Lawrence D. Gaspers§¶

From the ‡Departamento de Farmacologia, Universidade Federal de São Paulo 04044, UNIFESP-EPM, São Paulo 04044, Brazil and the §Department of Pharmacology and Physiology, New Jersey Medical School, Newark, New Jersey 07103

Cytosolic Ca^{2+} ($[Ca^{2+}]_i$) oscillations may be generated by the inositol 1,4,5-trisphosphate receptor (IP_3R) driven through cycles of activation/inactivation by local Ca^{2+} feedback. Consequently, modulation of the local Ca^{2+} gradients influences IP_3R excitability as well as the duration and amplitude of the $[Ca^{2+}]_i$ oscillations. In the present work, we demonstrate that the immunosuppressant cyclosporin A (CSA) reduces the frequency of IP_3-dependent $[Ca^{2+}]_i$ oscillations in intact hepatocytes, apparently by altering the local Ca^{2+} gradients. Permeabilized cell experiments demonstrated that CSA lowers the apparent IP_3 sensitivity for Ca^{2+} release from intracellular stores. These effects on IP_3-dependent $[Ca^{2+}]_i$ signals could not be attributed to changes in calcineurin activity, altered ryanodine receptor function, or impaired Ca^{2+} fluxes across the plasma membrane. However, CSA enhanced the removal of cytosolic Ca^{2+} by sarco-endoplasmic reticulum Ca^{2+}-ATPase (SERCA), lowering basal and interspike $[Ca^{2+}]_i$. In addition, CSA stimulated a stable rise in the mitochondrial membrane potential ($\Delta\Psi_m$), presumably by inhibiting the mitochondrial permeability transition pore, and this was associated with increased Ca^{2+} uptake and retention by the mitochondria during a rise in $[Ca^{2+}]_i$. We suggest that CSA suppresses local Ca^{2+} feedback by enhancing mitochondrial and endoplasmic reticulum Ca^{2+} uptake, these actions of CSA underlie the lower IP_3 sensitivity found in permeabilized cells and the impaired IP_3-dependent $[Ca^{2+}]_i$ signals in intact cells. Thus, CSA binding proteins (cyclophilins) appear to fine tune agonist-induced $[Ca^{2+}]_i$ signals, which, in turn, may adjust the output of downstream Ca^{2+}-sensitive pathways.

Immunosuppressants exert their activity by binding to immunophilins, an evolutionary conserved, but structurally heterogeneous family of proteins that shares a common enzymatic activity and pharmacological profile (1–3). All immunophilins described to date possess *cis-trans*-peptidylprolyl isomerase or rotamase activity, which has been implicated in the folding, assembly, and trafficking of target proteins *in vivo* (1, 2). The *cis-trans*-peptidylprolyl isomerase activity is inhibited by low concentrations of immunosuppressants. Based upon binding criteria, immunophilins are divided into two classes: (*a*) the cyclophilin family that selectively binds cyclosporin A (CSA)[1] and (*b*) the FK-506 binding proteins (FKBP), which bind to FK-506, its analogues, and rapamycin. Although the precise functions of immunophilins and their downstream targets remain to be determined, they have frequently been implicated in regulating a variety of Ca^{2+}-dependent pathways. The best characterized therapeutic action of CSA or FK-506 is the suppression of interleukin-2 gene transcription during antigen-induced T-lymphocyte activation. Specifically, CSA·cyclophilin or FK-506·FKBP complexes are targeted to and inhibit the catalytic activity of the Ca^{2+}/calmodulin-dependent protein phosphatase, calcineurin (4), thereby blocking the translocation of nuclear factor of activated T cells (3, 5).

In isolated mitochondria, CSA binds to cyclophilin D (CyP-D), which is believed to be a component of the mitochondrial permeability transition pore (PTP). Displacing CyP-D from its binding site favors the closed state of the pore (6–8). Recent evidence suggests that the PTP may be involved in Ca^{2+} signaling (9, 10), as well as necrotic and apoptotic cell death (11–15). Operating in a low conductance mode, the PTP is also proposed to furnish mitochondria with a fast Ca^{2+}-efflux mechanism (*i.e.* mitochondrial calcium-induced calcium-release) that, in turn, amplifies inositol 1,4,5-trisphosphate (IP_3)-dependent cytosolic calcium ($[Ca^{2+}]_i$) signals (9, 10).

Immunophilins may also modulate the Ca^{2+} release channels of the internal stores directly. FKBP12 forms tight complexes with both ryanodine receptors (RyRs) and IP_3 receptors (IP_3Rs) that are perturbed by FK-506 or rapamycin (16–19). Dissociation of the FKBP from the channels results in increased Ca^{2+} fluxes in response to caffeine or IP_3 (16, 18). This enhanced Ca^{2+} release can either be explained by destabiliza-

* This work was supported by a grant from the Fundação do Amparo à Pesquisa do Estado de São Paulo and by NIDDK, National Institutes of Health Grant DK38422. The costs of publication of this article were defrayed in part by the payment of page charges. This article must therefore be hereby marked "*advertisement*" in accordance with 18 U.S.C. Section 1734 solely to indicate this fact.

¶ To whom correspondence should be addressed: Dept. of Pharmacology and Physiology, New Jersey Medical School, 185 South Orange Ave., University Heights, Newark, NJ 07103. Tel.: 973-972-1142; Fax: 973-972-7950; E-mail: robbgald@umdnj.edu.

[1] The abbreviations used are: CSA, cyclosporin A; IP_3, inositol 1,4,5-trisphosphate; IP_3R, inositol 1,4,5-trisphosphate receptor; RyRs, ryanodine receptors; ER, endoplasmic reticulum; PE, phenylephrine; VP, vasopressin; MeVal-CS, *N*-methylvaline-cyclosporin; CyP-D, cyclophilin D; $[Ca^{2+}]_m$, mitochondrial matrix-free Ca^{2+} concentration; $[Ca^{2+}]_i$, cytosolic-free Ca^{2+} concentration; $[Ca^{2+}]_{ex}$, medium-free Ca^{2+} concentration; PMF, proton motive force; $\Delta\Psi_m$, mitochondrial membrane potential; FKBP, FK-506 binding protein; PTP, permeability transition pore; MES, 4-morpholineethanesulfonic acid; ICM, intracellular-like media; TMREE, tetramethylrhodamine ethyl ester; PKC, protein kinase C; Tg, thapsigargin; SERCA, sarco-endoplasmic reticulum Ca^{2+}-ATPase; BAPTA, 1,2-bis(2-aminophenoxy)ethane-*N,N,N′,N′*-tetraacetic acid; FK-506, tacrolimus; FCCP, carbonyl cyanide *p*-(tri-fluoromethoxy)phenyl-hydrazone; BTC, glycine, *N*-[3-(2-benzothiazolyl)-6-[2-[2-[bis(carboxymethyl)amino]-5-methylphenoxy]ethoxy]-2-oxo-2H-1-benzopyran-7-yl]-*N*-(carboxymethyl)-tetrapotassium salt; UNC, the mitochondrial inhibitors FCCP, rotenone, and oligomycin.

tion of the channel following FKBP12 dissociation (3, 16) or a change in the phosphorylation state, because FKBP12 also anchors calcineurin to the channel (17). Moreover, two ubiquitously expressed members of the cyclophilin family, *s*-cyclophilin and cyclophilin A, colocalize with or bind to the Ca^{2+} storage protein of the ER, calreticulin (20, 21). Therefore, this raises the possibility that cyclophilins may modulate Ca^{2+} storage properties of the ER and, indirectly, Ca^{2+} flux through the RyR and/or IP_3R. Taken together, there is a wealth of evidence that immunophilins can potentially activate or inhibit Ca^{2+}-dependent signal transduction by modifying the activity of diverse cellular targets.

Periodic oscillations or spikes in $[Ca^{2+}]_i$ are utilized by a wide range of extracellular stimuli (22–24) and are decoded by a host of downstream sensors (25–28). In non-excitable tissues, extracellular agonists mediate increases in $[Ca^{2+}]_i$ through the formation of the second messenger IP_3 and activation of intracellular Ca^{2+}-release channels (22–24, 29), which may in turn stimulate the influx of external Ca^{2+} to sustain the agonist signal and refill the internal stores (30). In hepatocytes, the agonist dose, which presumably determines the intracellular $[IP_3]$, sets the frequency of $[Ca^{2+}]_i$ spikes (*i.e.* frequency modulation). However, the positive feedback effect of $[Ca^{2+}]_i$ on IP_3R generates the rapid-rising phase of the $[Ca^{2+}]_i$ spike, which is essentially independent of the agonist dose. This Ca^{2+}-positive feedback is also thought to underlie the propagation of regenerative intracellular Ca^{2+} waves (24). We have previously suggested that the minimal prerequisites for generating oscillatory $[Ca^{2+}]_i$ signals are the concordant actions of Ca^{2+} and IP_3 on IP_3R function (31). Because Ca^{2+} is involved in both the activation and inactivation of the IP_3R (22–24), other Ca^{2+} transport mechanisms could exert profound effects on the dynamics and frequency of $[Ca^{2+}]_i$ signals by altering local Ca^{2+} gradients. Indeed, mitochondrial Ca^{2+} uptake can modulate IP_3 sensitivity by suppressing the local, positive feedback effects of Ca^{2+} on the IP_3R in hepatocytes (32).

In the present work, we have investigated the effects of CSA on IP_3-dependent $[Ca^{2+}]_i$ oscillations in hepatocytes. We demonstrate that CSA or its non-immunosuppressive analogue, *N*-methylvaline-cyclosporin (MeVal-CS), inhibits the frequency of IP_3-dependent $[Ca^{2+}]_i$ oscillations by simultaneously activating ER and mitochondrial Ca^{2+} uptake. We provide evidence that this activation suppresses local, positive Ca^{2+} feedback on the IP_3R and lowers IP_3R sensitivity. Thus, cyclophilins may play an essential role in determining the shape and frequency of IP_3-dependent $[Ca^{2+}]_i$ signals and, ultimately, the activity of downstream Ca^{2+}-sensitive targets by regulating cellular Ca^{2+} transport mechanisms.

EXPERIMENTAL PROCEDURES

Materials—Cyclosporin A and MeVal-CS were generous gifts from Novartis (Basil, Switzerland) and FK-506 from Fujisawa, Inc. Stock solutions were prepared in Me_2SO and diluted at least a 1000-fold in all experiments.

Cell Isolation and Culture—Hepatocytes were isolated by a two-step collagenase perfusion of livers from male Sprague-Dawley rats fed *ad libitum* as described previously (33). Isolated hepatocytes were stored on ice until assayed or maintained in primary culture for 1.5–3 h in Williams' E medium supplemented with 10% (v/v) fetal calf serum (complete WEM) as described previously (28). Hepatocytes used in confocal imaging experiments were cultured overnight in complete WEM containing insulin (14 nM). Prior to use, cells were incubated 30–40 min in a KR-HEPES buffer composed of (in millimolar): 121 NaCl, 25 Na-HEPES, 5 $NaHCO_3$, 4.7 KCl, 1.2 KH_2PO_4, 1.2 $MgSO_4$, 2 $CaCl_2$, 10 glucose, 0.1 sulfobromophthalein, and 0.25% (w/v) essentially fatty acid-free bovine serum albumin (fraction V, Sigma Chemical Co.), pH 7.4, at 37 °C. Where indicated in the figure legends, L-glutamate (5 mM) and pyruvate (1 mM) were also present during the incubation period.

Single Cell $[Ca^{2+}]_i$ Measurements—Ca^{2+} imaging experiments were preformed essentially as described previously (33, 34). Briefly, hepatocytes attached to collagen (5 $\mu g/cm^3$)-coated glass coverslips were loaded with fura-2 by incubation with 5 μM fura-2/AM for 15–30 min in a KR-HEPES buffer supplemented with 0.2% (w/v) Pluronic acid F-127. Fura-2-loaded hepatocytes were washed twice with KR-HEPES without dye or Pluronic acid and then transferred to a thermostatically regulated microscope chamber (37 °C). Fura-2 fluorescence images (excitation 340 and 380 nm, emission 420–600 nm) were acquired at 1- to 3-s intervals with a cooled charged-coupled device camera under computer control (33, 34). Calibration of fura-2 in terms of $[Ca^{2+}]_i$ was calculated from the 340/380 nm ratio after correcting for autofluorescence (35). Autofluorescence values were obtained at the end of each experiment by permeabilizing the cells with digitonin in an intracellular-like media containing a Ca^{2+}/EGTA buffer and Mg·ATP (35). The fura-2 calibration parameters were determined *in vitro* using a K_d value of 224 nM.

Single Cell Measurements of $\Delta\Psi$—Primary cultured hepatocytes were incubated with tetramethylrhodamine ethyl ester (TMREE, 5 nM) for 1–2 h in complete WEM then washed into a KR-HEPES buffer containing 5 nM TMREE. TMREE fluorescence images were collected using 548-nm excitation and 600-nm-long bandpass emission filter. The logarithm of TMREE fluorescence changes was normalized to the fluorescence intensity values obtained after collapsing the mitochondrial electrochemical gradient with 5 μM FCCP plus 5 μg/ml oligomycin.

Laser Scanning Confocal Microscopy—Simultaneous measurement of Mito Tracker Green and rhod-2 fluorescence were performed as described previously (33, 36). Briefly, overnight-cultured hepatocytes were incubated with 100 nM Mito Tracker Green for 1–2 h in complete WEM supplemented with 0.05% (w/v) Pluronic acid F-127. Cells were washed extensively and then loaded with rhod-2/AM (10 μM) in KR-HEPES buffer containing Pluronic acid F-127 (0.1% w/v) for 10 min at room temperature. Confocal images were acquired using a Bio-Rad MRC 600 laser scanning confocal microscope.

Mitochondrial Ca^{2+} Uptake in Permeabilized Hepatocyte—Hepatocytes (5 mg/ml cell protein) were washed once in a Ca^{2+}-free intracellular-like buffer (IB) composed of (in millimolar): 135 KCl, 15 NaCl, 1.2 $MgSO_4$, 1.2 KH_2PO_4, 10 HEPES, 10 MES, 5 glutamate, 1 pyruvate, 10 units/ml aprotinin, and 1 μg/ml each of leupeptin, antipain, and pepstatin A (pH 7.2 at 37 °C), and then stored on ice. Prior to use, cells were briefly centrifuged, suspended in prewarmed IB, and then incubated for 5 min in the presence of indicated drugs or vehicle. Incubations were carried out in a thermostatically regulated cuvette (37 °C) with continuous stirring. The cells were permeabilized with digitonin (25 μg/ml), and the medium was further supplemented with 5 mM phosphocreatine, 5 units/ml creatine phosphokinase, 2 mM ATP·K, 2 μM thapsigargin, and 10 μM BTC-free acid (Molecular Probes). BTC fluorescence (excitation 405 and 470 nm, emission 540) was monitored using a dual-wavelength excitation spectrofluorimeter. Calibration of BTC fluorescence ratio values was achieved by determining the minimum and maximum 405/470 ratios with EGTA/Tris and excess $CaCl_2$, respectively, at the end of each run (35). Medium-free Ca^{2+} concentration ($[Ca^{2+}]_{ex}$) was calculated assuming a K_d of 7 μM for BTC.

Mitochondrial Ca^{2+} Content in Intact Cells—Hepatocytes (5 mg/ml cell protein) were suspended in oxygenated, Ca^{2+}-containing KR-HEPES buffer and incubated for 15 min in a shaking water bath (37 °C). Where indicated in the figure legend, vasopressin or other drugs were included during the preincubation period. Following the preincubation, cell suspensions were rapidly centrifuged (60 s) and then suspended in a stirred cuvette containing Ca^{2+}-free KR-HEPES buffer plus 200 μM BAPTA-free acid and 10 μM fura-2-free acid. Rotenone (5 μM), antimycin A (5 μM), and oligomycin (5 μg/ml) were added to block mitochondrial respiration (not shown) followed by ionomycin (20 μM) to release compartmentalized Ca^{2+}. In some experiments, FCCP (5 μM) plus oligomycin (5 μg/ml) was included during the preincubation period to prevent mitochondrial Ca^{2+} accumulation. Fura-2 fluorescence was monitored by alternating excitation at 340 and 380 nm, and the emitted fluorescence was collected at 510 nm. The $[Ca^{2+}]_{ex}$ was calculated from the fura-2 ratio values using a K_d of 224 nM. The total ionomycin-releasable Ca^{2+} pool (buffered and free) was assessed to be predominately mitochondrial and calibrated by small additions of standardized $CaCl_2$ to the cuvette. Mitochondrial Ca^{2+} content was calculated assuming hepatocytes contain 0.24 mg of mitochondrial protein/mg of cell protein (37). Matrix Ca^{2+} determinations were performed in triplicate from two or three different cell preparations.

IP_3-induced Ca^{2+} Fluxes and Ca^{2+} Content of Internal Stores—Measurement of IP_3-induced Ca^{2+} release in permeabilized hepatocyte suspensions was performed essentially as described previously (38). Hepatocytes (5 mg/ml cell protein) were washed extensively in a Ca^{2+}-free Chelex-treated intracellular-like media (ICM) composed of (in millimo-

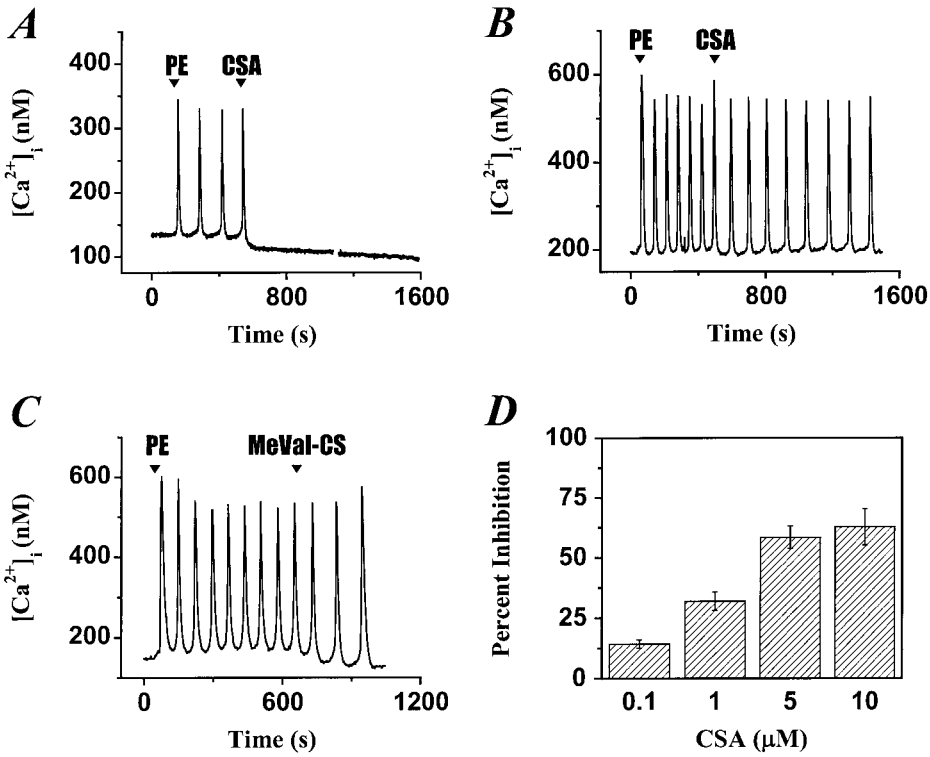

FIG. 1. **Cyclosporin A and its derivative, *N*-methylvaline-cyclosporin (MeVal-CS) inhibit IP_3-dependent $[Ca^{2+}]_i$ oscillations in hepatocytes.** In *A–C*, fura-2/AM-loaded primary cultured hepatocytes were stimulated with submaximal phenylephrine (*PE*) concentrations (0.5–5 μM), which induced typical baseline-separated $[Ca^{2+}]_i$ spikes. The addition of cyclosporin A (*CSA*, 5 μM) either abolished $[Ca^{2+}]_i$ oscillations (*A*) or reduced the frequency of $[Ca^{2+}]_i$ spiking (*B*). Complete inhibition of IP_3-dependent Ca^{2+} responses was only observed in cells displaying low frequency $[Ca^{2+}]_i$ spikes. MeVal-CS (5 μM), a CSA analogue that does not inhibit calcineurin, also inhibited IP_3-dependent $[Ca^{2+}]_i$ responses (*C*). CSA inhibited the frequency of PE-induced $[Ca^{2+}]_i$ oscillations in a concentration-dependent manner (*D*; n = 30–90 cells/condition). In this and all subsequent figures, the *arrows* indicate the time of addition. The indicated compound was then present continuously through the rest of the experiment.

lar): 130 KCl, 10 NaCl, 1.0 KH_2PO_4, 20 HEPES, 20 Tris, 5 glutamate, 1 pyruvate, 10 units/ml aprotinin, and 1 μg/ml each of leupeptin, antipain, and pepstatin A (pH 7.2 at 37 °C), then stored on ice. Prior to the experiment, cells were washed into prewarmed ICM supplemented with phosphocreatine (5 mM) and fura-2-free acid (5 μM) then incubated for 5 min in a stirred thermostatted cuvette. When indicated in the figure legends, CSA (5 μM) or Me_2SO vehicle (0.1%, v/v) was included during the preincubation period. Cells were permeabilized with digitonin (40 μg/ml) in the presence of 5 units/ml creatine phosphokinase for 2 min followed by addition of 2 mM Mg·ATP to initiate Ca^{2+} uptake. In some experiments, mitochondrial Ca^{2+} uptake was inhibited by adding rotenone (5 μM) plus oligomycin (5 μg/ml) prior to permeabilization. fura-2 fluorescence changes were monitored as described in the previous section. IP_3-induced Ca^{2+} release was normalized to the size of the ionomycin-releasable Ca^{2+} pool. In parallel experiments, the Ca^{2+} content of the ionomycin-sensitive Ca^{2+} store was determined. After cell permeabilization, rotenone, oligomycin, FCCP (0.5 μM), and Mg·ATP were added and the cell suspension incubated for 15 min. FCCP was included to help facilitate the release of stored mitochondrial matrix Ca^{2+}. The size of the ionomycin-releasable Ca^{2+} store was calibrated by small additions of standardized $CaCl_2$ to the cuvette. Under these conditions, the size of the thapsigargin-sensitive Ca^{2+} pool was 90–95% of the ionomycin-sensitive Ca^{2+} pool.

Protein Determination—Protein content was determined by alkaline biuret assay using the methods described by the manufacture (Sigma).

Statistical Analysis—Unless otherwise stated in the text, all experiments were repeated with at least three separate hepatocyte preparations. Data are presented as means ± S.E. for the number of separate hepatocyte preparations shown in parentheses. Significance of differences from the relevant controls was calculated by Student's *t* test.

RESULTS

CSA Inhibits $[Ca^{2+}]_i$ Oscillations in Single Hepatocytes—Stimulation of rat hepatocytes with submaximal concentrations of IP_3-forming agonists induces a series of baseline-separated $[Ca^{2+}]_i$ oscillations or spikes. The frequency of the $[Ca^{2+}]_i$ oscillations is dependent upon the agonist concentration and remains constant for a given dose over the time course of the experiment (34). The *traces* in Fig. 1, *A–C*, and Fig. 2*A* illustrate typical, single cell $[Ca^{2+}]_i$ responses to submaximal concentrations of phenylephrine (PE), an IP_3-forming agonist. Addition of CSA (5 μM) to ongoing PE-induced $[Ca^{2+}]_i$ oscillations either completely inhibited the $[Ca^{2+}]_i$ response (Fig. 1*A*) or significantly slowed the frequency of the $[Ca^{2+}]_i$ oscillations (Figs. 1*B* and 2*A*). In control experiments, the solvent, Me_2SO (0.2%; v/v), did not effect the frequency or shape of agonist-induced $[Ca^{2+}]_i$ spikes (not shown). CSA reduced the frequency of PE-induced Ca^{2+} oscillations in a concentration-dependent manner, with half-maximal inhibition at 3.4 μM (Fig. 1*D*). This effect was reversed upon washout of the drug (not shown). Moreover, CSA caused similar inhibition of oscillatory $[Ca^{2+}]_i$ signals induced by submaximal vasopressin (VP) concentrations (not shown).

Note that CSA resulted in an immediate, but small, decrease in inter-spike $[Ca^{2+}]_i$ (Figs. 1 and 2) that persisted throughout the time course of the experiment (20–30 min). This effect also occurred in the absence of agonist (see Fig. 4*A*). In naive cells, CSA decreased basal $[Ca^{2+}]_i$ by 30 ± 1.0 nM (mean ± S.E.; n = 250 cells, five cell preparations). These data suggest that CSA may promote Ca^{2+} clearance from the cytosol, which could be one of the underlying mechanisms suppressing the frequency of $[Ca^{2+}]_i$ spikes. The effect of CSA on basal $[Ca^{2+}]_i$ was investigated in length and discussed in more detail below.

Another possible mechanism of action for the CSA·cyclophilin complex is the inhibition of calcineurin (3, 5), which is known to increase PKC-dependent phosphorylation of IP_3Rs in isolated cerebellar microsomes (17). The CSA derivative, MeVal-CS, binds cyclophilins with a similar efficacy to CSA (39), but the complex cannot inhibit calcineurin activity (40–42). The addition of MeVal-CS (5 μM) also inhibited the frequency of PE-induced $[Ca^{2+}]_i$ oscillations (Fig. 1*C*) in a concentration-dependent manner (data not shown) with a potency similar to CSA. Furthermore, a 10- to 15-min preincubation with a PKC inhibitor, bisindolylmaleimide-1 (0.1–1.0 μM), did not block the inhibitory effects of CSA on PE-induced $[Ca^{2+}]_i$ responses (data not shown). Taken together, these data suggest that CSA-induced inhibition of IP_3-dependent Ca^{2+} signals is not mediated by either PKC or calcineurin.

In some cell types, IP_3-induced Ca^{2+} release has been proposed to trigger calcium-induced calcium-release via RyRs. Specific [^{3}H] ryanodine binding to isolated hepatic microsomes

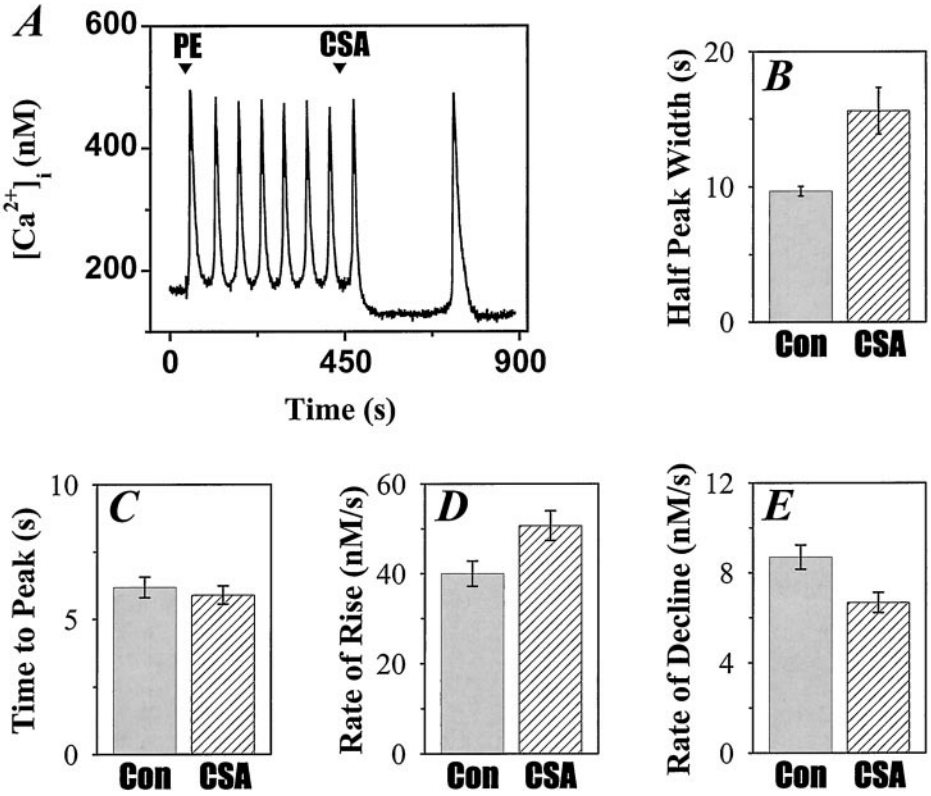

FIG. 2. **Cyclosporin A modifies the shape and kinetics of IP_3-dependent $[Ca^{2+}]_i$ spikes.** Rapid data acquisition was employed to assess the effect of CSA on the shape and kinetics of PE-induced $[Ca^{2+}]_i$ spikes. The *trace* in *A* illustrates a typical single cell $[Ca^{2+}]_i$ response to submaximal PE stimulation and the subsequent addition of CSA (5 μM). Note that CSA decreases basal $[Ca^{2+}]_i$ and broadens the width of the $[Ca^{2+}]_i$ spike. The data in *B–D* represent the means ± S.E. (n = 40 cells, three cell preparations). *B*, CSA significantly increased the half-peak width of PE-induced $[Ca^{2+}]_i$ spikes ($p < 0.001$). The half-peak width is the width of the $[Ca^{2+}]_i$ spike, in seconds, measured at half-peak height. *C*, CSA does not effect the time to peak of the $[Ca^{2+}]_i$ transient. CSA significantly increased the rate of $[Ca^{2+}]_i$ rise ($p < 0.001$; *D*) while decreasing the rate of decay ($p < 0.001$; *E*). The rates of rise and decay of the $[Ca^{2+}]_i$ spike were measured as described previously (34).

has been reported, and RyR inhibitors appear to inhibit IP_3-dependent Ca^{2+} signaling in isolated intact hepatocytes (43). To rule out a direct CSA effect on RyRs, hepatocytes were preincubated for 10–15 min with 100 μM ryanodine prior to PE stimulation. In these experiments, CSA still inhibited IP_3-dependent $[Ca^{2+}]_i$ responses suggesting that RyRs are not involved in the drug's action (data not shown).

CSA Alters the Kinetics of IP_3-dependent $[Ca^{2+}]_i$ Spikes—Despite the lower basal $[Ca^{2+}]_i$, peak amplitude and time to peak were the same before and after CSA addition (Fig. 2, *A* and *C*), although there was a small, but significant, increase in the rate of Ca^{2+} rise ($p < 0.001$; Fig. 2*D*). The most obvious effect of CSA on the kinetics of the individual $[Ca^{2+}]_i$ spikes was to slow the rate of decline ($p < 0.001$), resulting in a prolongation of the Ca^{2+} transient (Fig. 2, *B* and *E*). To investigate the mechanism for these effects on Ca^{2+} removal from the cytosol, we examined the effects of CSA on Ca^{2+} transport across the plasma membrane, as well as Ca^{2+} uptake into internal stores.

CSA Does Not Affect Ca^{2+} Transport Across the Plasma Membrane—Maximal VP stimulation rapidly releases Ca^{2+} from IP_3-sensitive stores and in the presence of extracellular Ca^{2+} results in a sustained elevation in $[Ca^{2+}]_i$ (Fig. 3*A*). This sustained phase of $[Ca^{2+}]_i$ increase is dependent upon Ca^{2+} influx and is set by the balance between Ca^{2+} influx and efflux across the plasma membrane (*cf.* Fig. 3*D*). In Fig. 3*A*, BAPTA was added during the sustained rise in $[Ca^{2+}]_i$ to abruptly inhibit Ca^{2+} influx. The initial rate of Ca^{2+} clearance from the cytosol, which mostly reflects Ca^{2+} efflux mechanisms, was unaltered by CSA pretreatment (Fig. 3*A*, *gray trace*). An alternative method to assess efflux rates is to measure the appearance of Ca^{2+} in the external buffer after mobilizing internal stores. In cell suspension experiments, CSA pretreatment did not effect the rate of Ca^{2+} efflux elicited by the addition of maximal concentrations of either VP or thapsigargin (Tg) (not shown).

In Fig. 3*B*, hepatocytes were stimulated with maximal VP for 10 min in the absence of extracellular Ca^{2+} to activate capacitative Ca^{2+} influx channels (not shown). CSA preincubation (*gray trace*) did not alter the rate nor the extent of the mean $[Ca^{2+}]_i$ response evoked after restoring extracellular Ca^{2+}, indicating no effect of CSA on Ca^{2+} influx. Thapsigargin was also used to elevate $[Ca^{2+}]_i$ independent of IP_3 formation. The addition of maximal Tg concentrations resulted in a slow rise in $[Ca^{2+}]_i$ that reached a plateau after 5 min in Ca^{2+}-containing buffer. Neither CSA (Fig. 3*C*) nor Me_2SO (not shown) affected the sustained elevation in $[Ca^{2+}]_i$. Moreover, CSA did not alter the initial rate of Mn^{2+}-dependent quench of intracellular fura-2 fluorescence in Tg-pretreated cells; the quench rate was 0.33 ± 0.05%/s and 0.37 ± 0.06%/s in CSA- and Me_2SO-treated cells, respectively ($p > 0.1$, $n = 4$). Locally high $[Ca^{2+}]$ gradients evoked by either VP or Tg stimulation could potentially mask the effect of CSA on plasma membrane Ca^{2+} transport. To rule out this possibility, fura-2-loaded hepatocytes were preincubated 2 min in a Ca^{2+}-free buffer and then challenged with maximal VP. In the absence of extracellular Ca^{2+}, maximal VP stimulation evoked a transient $[Ca^{2+}]_i$ response due to store depletion and lack of Ca^{2+} influx (Fig. 3*D*). Ca^{2+} influx was initiated by the addition of 0.5 mM $CaCl_2$ (*Lo Ca^{2+}*) to the external medium. This concentration of extracellular Ca^{2+} did not saturate the Ca^{2+} influx pathway, as evidenced by an abrupt increase in $[Ca^{2+}]_i$ upon raising extracellular Ca^{2+} to 2 mM (*Hi Ca^{2+}*). The addition of CSA after partially restoring extracellular Ca^{2+} levels had only a negligible effect on $[Ca^{2+}]_i$, in fact Ca^{2+} rose slightly after drug addition. Taken together, these data are consistent with CSA having no effect on Ca^{2+} influx or efflux across the plasma membrane in hepatocytes.

Effect of CSA on Basal $[Ca^{2+}]_i$—The addition of BAPTA (5 mM) to completely chelate extracellular Ca^{2+} and inhibit Ca^{2+} influx had no additional effects on $[Ca^{2+}]_i$ in CSA-treated hepatocytes (Fig. 4*A*). When BAPTA was added prior to CSA, $[Ca^{2+}]_i$ slowly decreased and this rate was enhanced upon CSA addition (Fig. 4*B*). In parallel experiments, the protonophore, FCCP, was added to collapse mitochondrial proton motive force

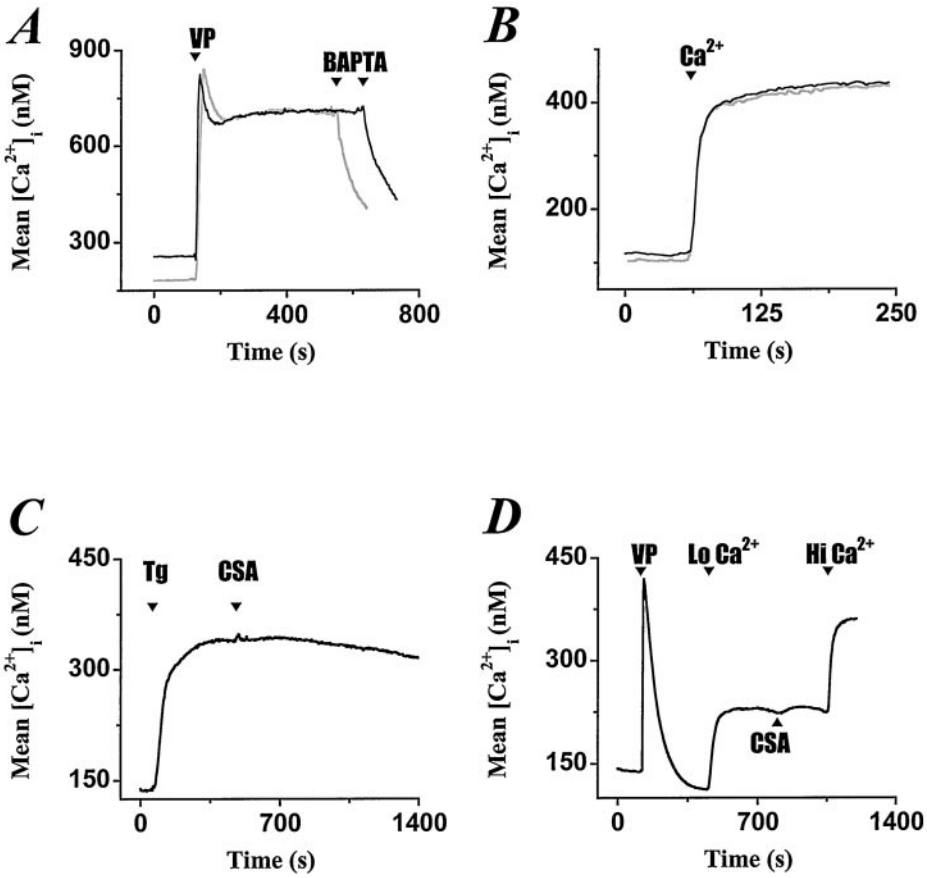

FIG. 3. **Cyclosporin A does not affect Ca^{2+} fluxes across the plasma membrane.** In *A* and *B*, hepatocytes were preincubated with CSA (5 μM, *gray traces*) or Me_2SO (0.1% v/v, *black traces*) 5 min prior to maximal vasopressin (*VP*) stimulation in the presence (*A*) or absence (*B*) of extracellular Ca^{2+}. In *A*, BAPTA (5 mM) was added during the sustained elevation in $[Ca^{2+}]_i$ to estimate the rate of Ca^{2+} efflux, whereas the rate of Ca^{2+} influx was measured after depleting internal stores (2 mM Ca^{2+}, *B*). *C* shows the lack of effect of CSA (5 μM) on the thapsigargin (*Tg*)-induced sustained rise in $[Ca^{2+}]_i$. In *D*, cultured hepatocytes were washed into a Ca^{2+}-free extracellular buffer just prior to data acquisition. The additions are 50 nM VP, 0.5 mM $CaCl_2$ (*Lo Ca^{2+}*), 5 μM CSA, and 1.5 mM $CaCl_2$ (*Hi Ca^{2+}*). All *traces* represent the mean $[Ca^{2+}]_i$ responses of all the cells in the imaging field (50–100 cells) and are typical of at least three experiments from different cell preparations.

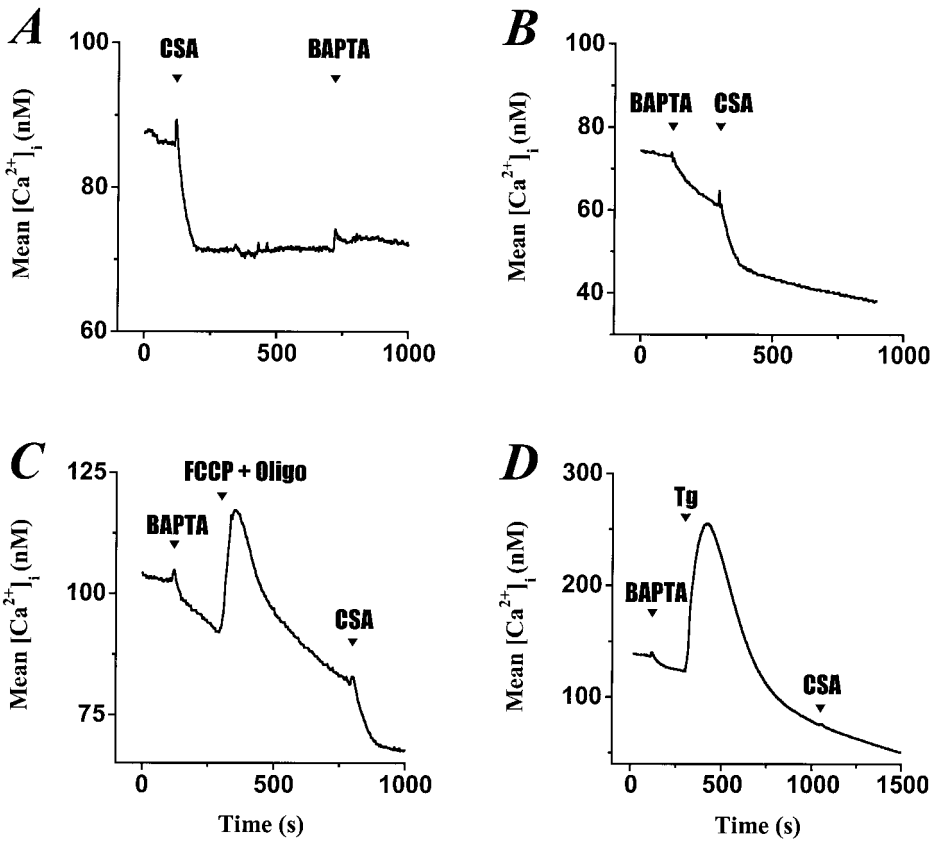

FIG. 4. **Effect of cyclosporin A on basal $[Ca^{2+}]_i$.** The effect of CSA (5 μM) on basal $[Ca^{2+}]_i$ before (*A*) or after (*B*) chelating extracellular Ca^{2+} with BAPTA (5 mM). In *C*, the protonophore, FCCP (5 μM), plus oligomycin (*Oligo*, 1 μg/ml) was added to inhibit mitochondrial Ca^{2+} transport. *D*, the effect of CSA on basal $[Ca^{2+}]_i$ is completely blocked by thapsigargin (*Tg*) addition. *Traces* represent the mean $[Ca^{2+}]_i$ responses of all the cells in the imaging field (50–100 cells) and are typical of at least three experiments from different cell preparations.

(PMF), thus inhibiting mitochondrial Ca^{2+} uptake. Oligomycin (*Oligo*) was included in these experiments to limit FCCP-stimulated ATP hydrolysis (33). Collapsing mitochondrial PMF released matrix Ca^{2+} stores and transiently raised $[Ca^{2+}]_i$ (Fig. 4*C*). Subsequent CSA addition still stimulated a robust decrease in $[Ca^{2+}]_i$ (Fig. 4*C*), indicating that CSA does not stim-

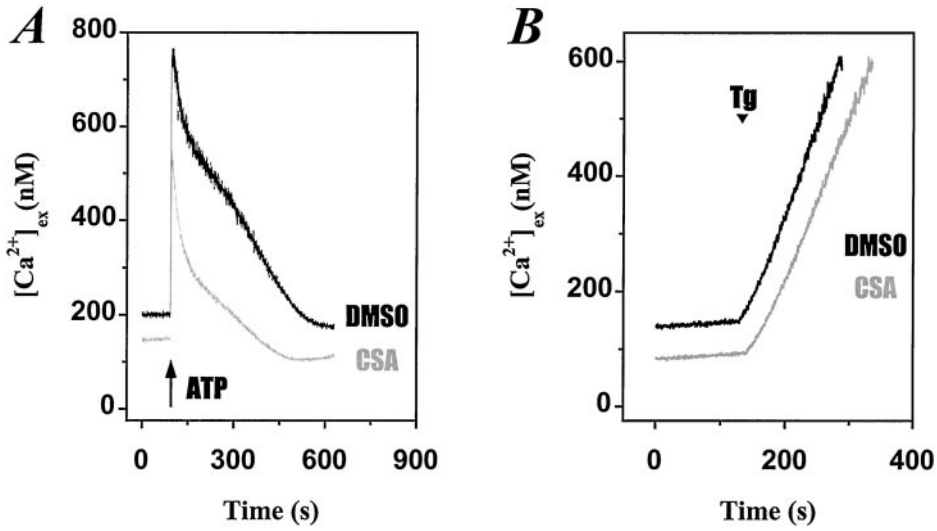

FIG. 5. **Effect of cyclosporin A on ATP-dependent Ca^{2+} uptake into internal stores.** Intact hepatocytes suspensions were pretreated 5 min with CSA (5 μM, *gray traces*) or Me_2SO (*black traces*) prior to permeabilization. Cells were digitonin-permeabilized in a Chelex-treated ICM containing mitochondrial inhibitors and fura-2-free acid (see "Experimental Procedures"). The addition of exogenous ATP plus Ca^{2+} rapidly elevates medium Ca^{2+} levels followed by ATP-dependent Ca^{2+} uptake into internal stores (*A*). In parallel experiments, thapsigargin (*Tg*; 2 μM) was added after ATP-dependent Ca^{2+} uptake to assess the passive Ca^{2+} leak rate from internal stores (*B*). Data shown are typical $[Ca^{2+}]_{ex}$ responses from three to four different cell preparations.

ulate Ca^{2+} uptake into the mitochondria under basal conditions. This is not surprising given the fact that the mitochondrial uniporter has a low affinity for Ca^{2+} (*i.e.* $K_{0.5}$ = 5–10 μM; see Refs. 44, 45). By contrast, inhibiting SERCA activity with Tg completely blocked the effect of CSA on basal $[Ca^{2+}]_i$ (Fig. 4*D*). Furthermore, when MeVal-CS was substituted for CSA, qualitatively similar results were obtained for each experimental protocol shown in Fig. 4, indicating that these effects were independent of calcineurin (not shown). These data suggest that the decrease in basal $[Ca^{2+}]_i$ is mediated by Ca^{2+} uptake into internal stores via SERCA.

Permeabilized hepatocytes suspensions were used to further investigate the effects of CSA on Ca^{2+} uptake into internal stores in the presence of inhibitors to block mitochondrial Ca^{2+} transport. Fig. 5*A* shows that, in the presence of endogenous ATP, CSA-treated hepatocytes consistently buffered medium-free Ca^{2+} concentrations ($[Ca^{2+}]_{ex}$) to lower values when compared with Me_2SO-treated cells. Addition of exogenous ATP and Ca^{2+} (*arrow*) resulted in a prompt increase of $[Ca^{2+}]_{ex}$, followed by Ca^{2+} uptake into Tg-sensitive stores. The CSA-treated cells consistently showed an enhanced rate of Ca^{2+} uptake and buffered the medium to lower Ca^{2+} levels (Fig. 5*A*). Under these conditions, the $[Ca^{2+}]_{ex}$ was 175 ± 14 nM and 133 ± 12 nM in Me_2SO-pretreated and CSA-pretreated hepatocyte suspensions, respectively, after ATP-dependent Ca^{2+} uptake (mean ± S.E.; n = 3). Once steady-state Ca^{2+} uptake reached completion, ionomycin was used to check the final store size. Despite enhancing the rate of Ca^{2+} uptake, the ionomycin-sensitive Ca^{2+} pool was not significantly increased in the presence of CSA. The final steady-state Ca^{2+} pool was 2.75 ± 0.1 and 2.88 ± 0.1 nmol/mg of protein in the absence and presence of CSA, respectively ($p > 0.1$; n = 3).

In parallel experiments, Tg was added to assess the passive Ca^{2+} leak rate from internal stores (Fig. 5*B*). CSA pretreatment did not affect the rate of Ca^{2+} leak (*gray trace*); $[Ca^{2+}]_{ex}$ increased 5.8 ± 1.1 nM/s and 4.4 ± 0.6 nM/s in Me_2SO- and CSA-treated cells, respectively ($p > 0.1$; mean ± S.E., n = 3). Under both conditions, the size of the Tg-sensitive Ca^{2+} pool was 90–95% of the ionomycin-releasable pool, suggesting that CSA does not significantly stimulate Ca^{2+} uptake into Tg-insensitive stores. Taken together, these data suggest that CSA simulates Tg-sensitive Ca^{2+} pumps to enhance the rate of Ca^{2+} clearance from the cytosol and lower the final set point for basal $[Ca^{2+}]_i$. Furthermore, these effects are independent of calcineurin and point to a role for an ER-associated cyclophilin that regulates SERCA activity.

Effect of CSA on IP_3-induced Ca^{2+} Release from Internal Stores—The effects of CSA on SERCA activity would presumably alter local Ca^{2+} gradients, decreasing the positive feedback effects of Ca^{2+} on the IP_3R. To test for a shift in IP_3R sensitivity, we measured the effects of CSA on IP_3-induced Ca^{2+} fluxes in permeabilized hepatocytes. In the presence of energized mitochondria, CSA decreased both the sensitivity of the internal stores to IP_3 and the maximum size of the IP_3-sensitive Ca^{2+} store (Fig. 6*A*). The half-maximal response (EC_{50}) to IP_3 increased from 128 nM in Me_2SO-treated cells to 179 nM after CSA treatment. The $[Ca^{2+}]_{ex}$ prior to IP_3 addition was lower in the CSA-treated cells (see Fig. 5*A*). The small differences in $[Ca^{2+}]_{ex}$ are in the range of the half-maximal effects of Ca^{2+} on the activation of IP_3Rs in hepatocytes (46), and thus could explain the shift in IP_3 sensitivity. To exclude this possibility, small amounts of Ca^{2+} were added to the medium until essentially no further Ca^{2+} uptake occurred and $[Ca^{2+}]_{ex}$ rose to similar levels in both Me_2SO- and CSA-treated hepatocytes. At equivalent free Ca^{2+} levels, IP_3-induced Ca^{2+} fluxes were still smaller in CSA-treated cells, indicating that the shift in receptor sensitivity is not mediated by the different baseline $[Ca^{2+}]_{ex}$ levels (not shown). Moreover, including ryanodine (100–200 μM) in the permeabilization buffer did not change the effects of CSA on IP_3R sensitivity, suggesting that RyRs are not involved in the action of CSA (not shown).

The most striking effect of CSA treatment is the decrease in the size of the IP_3-sensitive Ca^{2+} pool. The blunted Ca^{2+} fluxes cannot be explained by differences in pool size, because the ionomycin-releasable Ca^{2+} pool is not significantly increased in CSA-treated cells (see text). Moreover, CSA did not modify the initial rate of Ca^{2+} release at maximal IP_3 concentrations, the fura-2 ratio increased 0.94 ± 0.05 unit/s in Me_2SO-treated cells verses 0.89 ± 0.05 unit/s in CSA-treated cells ($p > 0.2$; n = 3). The lack of effect on initial rates of IP_3-induced Ca^{2+} release, coupled with the increased rate of $[Ca^{2+}]_i$ rise in the intact cells (Fig. 2*D*), suggest that CSA did not directly inhibit Ca^{2+} flux through the IP_3R.

CSA has been reported to increase the size of the mitochondrial Ca^{2+} pool in intact cells (47, 48). An enhanced rate of mitochondrial Ca^{2+} uptake could buffer IP_3-induced $[Ca^{2+}]_{ex}$ responses. To test this possibility, hepatocyte suspensions were treated with mitochondrial inhibitors prior to digitonin permeabilization. Blocking mitochondrial Ca^{2+} uptake resulted in a less pronounced rightward shift in the IP_3 concentration response curve but did not eliminate the effects of CSA on the IP_3-sensitive Ca^{2+} store size (Fig. 6*B*). The EC_{50} values were 128 and 148 nM in the absence and presence of CSA, respectively. These data suggest that the mitochondria are not in-

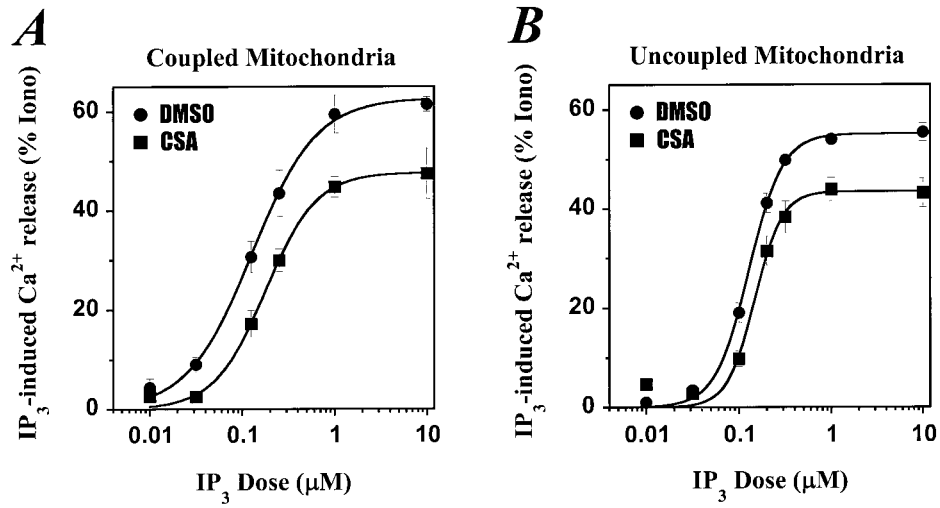

FIG. 6. **Concentration response curves for IP_3-induced Ca^{2+} release.** Hepatocyte suspensions were washed extensively to removed extracellular Ca^{2+} then suspended in Chelex-treated ICM supplemented with 5 μM cyclosporin A (*CSA*, ■) or Me_2SO (0.1% v/v, ●) and incubated 5 min in a stirred cuvette. Cells were then digitonin-permeabilized in the presence of an ATP-regenerating system plus glutamate and pyruvate as described under "Experimental Procedures." Fura-2-free acid was used to measure IP_3-induced Ca^{2+} fluxes, which are normalized to the magnitude of the ionomycin-sensitive Ca^{2+} store (*% Iono*). *A*, effect of CSA on the IP_3 concentration response curve in the presence of respiring, coupled mitochondria. *B*, hepatocyte suspensions were treated with rotenone and oligomycin prior to permeabilization to block mitochondrial Ca^{2+} uptake. The data are the means ± S.E. (n = 3–7 hepatocyte preparations). The data points were fit to the Hill equation.

volved in suppressing the magnitude of IP_3-induced Ca^{2+} fluxes but may partially mediate the reduction in IP_3R sensitivity.

The most likely explanation for the apparent smaller IP_3-sensitive Ca^{2+} pool in CSA-treated cells is the enhanced rate of Ca^{2+} clearance by SERCA, which is expected to buffer the $[Ca^{2+}]_{ex}$ responses. Moreover, the findings described above are consistent with both SERCA activity and the mitochondria acting synergistically to inhibit IP_3-induced Ca^{2+} release in CSA-treated hepatocytes. This effect could be mediated by suppression of the positive feedback effects of Ca^{2+} on the IP_3R. To determine the role of the mitochondria in this process, we investigated the effects of CSA on mitochondrial Ca^{2+} transport mechanisms.

Effect of CSA on Mitochondrial Transport Mechanisms—Hepatocytes were maintained in primary culture overnight then co-loaded with Mito Tracker Green, to visualize the mitochondria, and the Ca^{2+}-sensitive indicator, rhod/2-AM to measure mitochondrial matrix-free Ca^{2+} concentrations ($[Ca^{2+}]_m$) (33, 36). Cells were simulated with maximal VP concentrations and $[Ca^{2+}]_m$ responses monitored by confocal microscopy. As reported previously (33, 36), VP stimulation rapidly increased rhod-2 fluorescence in individual mitochondria (Fig. 7*A*). Analysis of rhod-2 fluorescence changes (500–1000 mitochondria per cell) revealed that CSA pretreatment increased the rate of rise in $[Ca^{2+}]_m$ after VP stimulation from 8.3 ± 2.5%/s to 21.7 ± 5.8%/s ($p < 0.05$; n = 2–4 cells). It is worth re-emphasizing that CSA did not alter the rate nor the magnitude of VP-induced $[Ca^{2+}]_i$ responses (Fig. 3*A*), indicating that rhod-2 is reporting a differential effect on mitochondrial Ca^{2+} uptake *in situ*. No significant differences in the magnitude of $[Ca^{2+}]_m$ responses could be detected with rhod-2; fluorescence intensities increased 210 ± 34% and 240 ± 7% above basal values in the absence and present of CSA, respectively ($p > 0.5$). However, this may reflect saturation of rhod-2.

The total accumulation of mitochondrial matrix Ca^{2+} during a rise in $[Ca^{2+}]_i$ was measured in intact hepatocyte suspensions (49) pretreated with maximal VP (Fig. 7*B*) or VP plus Tg (Fig. 7*C*). Cells were quickly washed into a BAPTA-containing medium plus fura-2-free acid, and the compartmentalized Ca^{2+} was released by ionomycin (*Iono*). CSA significantly increased the amount of Ca^{2+} accumulated by the mitochondria during VP stimulation (Fig. 7*B*). Under these conditions, the ionomycin-releasable Ca^{2+} pool predominately originated from the mitochondria, because the same effect was also observed in cells treated with VP plus Tg (Fig. 7*C*). Moreover, greater than 90% of the ionomycin-releasable Ca^{2+} pool was blocked by including mitochondrial inhibitors during the preincubation period (Fig. 7C, *FCCP*). In the presence of VP alone, CSA increased mitochondrial Ca^{2+} content from 3.9 ± 0.7 to 12.6 ± 1.9 nmol/mg of mitochondrial protein ($p < 0.05$; mean ± S.E., n = 3). In VP- plus Tg-treated hepatocytes, matrix Ca^{2+} content was 13.6 ± 0.8 and 21.2 ± 1.3 nmol/mg of mitochondrial protein in the absence and presence of CSA, respectively ($p < 0.05$; mean ± S.E., n = 3).

CSA is known to decrease the open probability of the mitochondrial PTP (6), which in some cell types leads to an increase in mitochondrial membrane potential ($\Delta\Psi_m$) (50, 51). Because the initial rate of mitochondrial Ca^{2+} uptake is proportional to the magnitude of $\Delta\Psi_m$ (52), we explored the possibility that CSA mediates its effect through changes in $\Delta\Psi_m$. We have shown previously that real-time measurement of $\Delta\Psi_m$ can be achieved in intact cells using the fluorescent indicator, tetramethylrhodamine ethyl ester (TMREE) (33, 36). Addition of CSA to naive cells caused a stable increase in the mean TMREE fluorescence, indicating a rise in $\Delta\Psi_m$ corresponding to a 1–2% increase in the logarithm of the fluorescence ratio (Fig. 7*D*). This observation is consistent with a constitutively active mitochondrial PTP or megachannel operating in a low conductance mode (*i.e.* flickering). For comparison, hepatocytes were subsequently treated with K^+/H^+ ionophore, nigericin (*Nig*, Fig. 7*D*), that slowly abolishes the mitochondrial proton gradient converting the free energy into $\Delta\Psi_m$ (36) and, thus, hyperpolarizes the mitochondrial inner membrane.

To further investigate the effects of CSA on mitochondrial Ca^{2+} transport without the interference of plasma membrane Ca^{2+} transporters, we returned to the permeabilized hepatocyte preparation. In these experiments, Tg was added to preclude any CSA-dependent effects on the SERCA pumps and a low affinity Ca^{2+} indicator dye (BTC; K_d = 7 μM) was employed to measure $[Ca^{2+}]_{ex}$. A $CaCl_2$ pulse (30 nmol/mg of cell protein) to pre-energized mitochondria initiated Ca^{2+} uptake (Fig. 8*A*) which was indicated by a decrease in $[Ca^{2+}]_{ex}$ following the Ca^{2+} pulse. A 5-min preincubation with CSA (5 μM) prior to

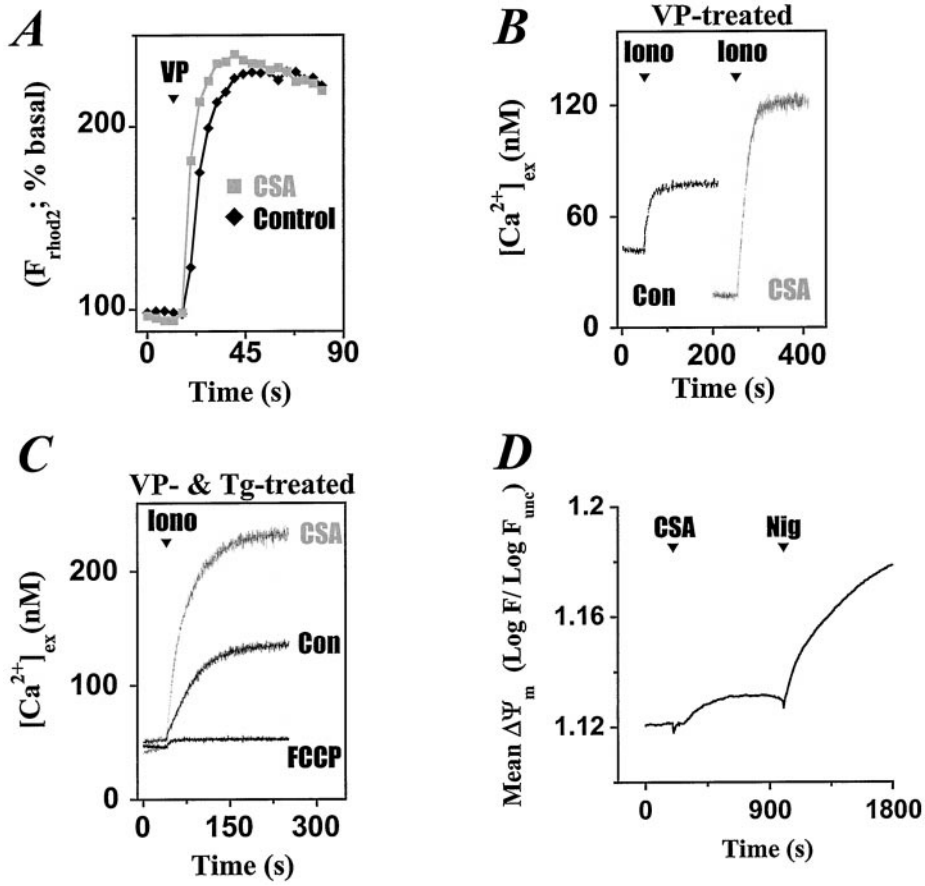

FIG. 7. **Cyclosporin A enhances mitochondrial Ca^{2+} uptake and increases $\Delta\Psi_m$ in intact hepatocytes.** *A*, rhod-2 fluorescence changes during maximal vasopressin (*VP*, 100 nM) stimulation. Dual-wavelength confocal microscopy was used to simultaneously monitor Mito Tracker Green fluorescence, to visualize mitochondrial structure, and rhod-2 to measure $[Ca^{2+}]_m$ responses (33, 36). CSA (5 μM, *gray trace*) was present 5 min prior to data acquisition. The data represent the mean rhod-2 fluorescence from all the mitochondria within the cell. *B* and *C*, effect of CSA on the total mitochondrial Ca^{2+} content. Intact hepatocytes were suspended in Ca^{2+}-containing KR-HEPES buffer supplemented with (*B*) VP (100 nM) or (*C*) VP plus thapsigargin (2 μM, *Tg*) and gently shaken for 15 min in the presence or absence of CSA (5 μM). Cell suspensions were then washed into Ca^{2+}-free KR-HEPES buffer supplemented with BAPTA and fura-2-free acid followed by ionomycin (*Iono*) to release compartmentalized Ca^{2+}. In some experiments, FCCP plus oligomycin was included during the preincubation period to prevent mitochondrial Ca^{2+} accumulation (*C*, FCCP). *D*, typical mean mitochondrial membrane potential ($\Delta\Psi_m$) response in TMREE-loaded hepatocytes. Cells were challenged with CSA (5 μM) followed by the K^+/H^+ ionophore, nigericin (*Nig*, 1 μM). The logarithm of TMREE fluorescence intensity changes were normalized as described under "Experimental Procedures."

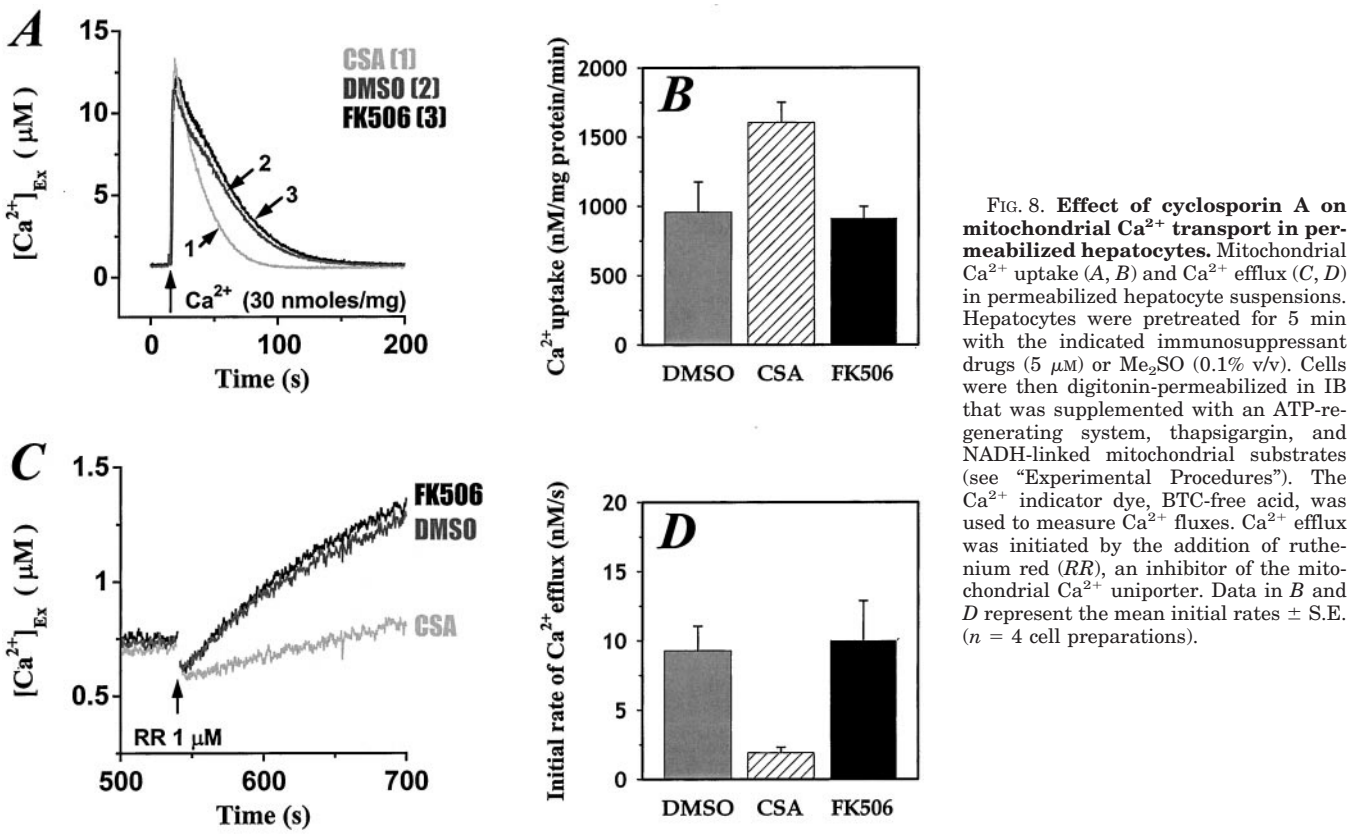

FIG. 8. **Effect of cyclosporin A on mitochondrial Ca^{2+} transport in permeabilized hepatocytes.** Mitochondrial Ca^{2+} uptake (*A*, *B*) and Ca^{2+} efflux (*C*, *D*) in permeabilized hepatocyte suspensions. Hepatocytes were pretreated for 5 min with the indicated immunosuppressant drugs (5 μM) or Me_2SO (0.1% v/v). Cells were then digitonin-permeabilized in IB that was supplemented with an ATP-regenerating system, thapsigargin, and NADH-linked mitochondrial substrates (see "Experimental Procedures"). The Ca^{2+} indicator dye, BTC-free acid, was used to measure Ca^{2+} fluxes. Ca^{2+} efflux was initiated by the addition of ruthenium red (*RR*), an inhibitor of the mitochondrial Ca^{2+} uniporter. Data in *B* and *D* represent the mean initial rates ± S.E. (n = 4 cell preparations).

digitonin permeabilization significantly enhanced the initial rate of mitochondrial Ca^{2+} uptake (Fig. 8, *A* and *B*; $p < 0.05$), consistent with the rhod-2 measurements in intact hepatocytes (Fig. 7*A*). Ruthenium red (1 μM) was added after Ca^{2+} uptake to block the mitochondrial uniporter, thus permitting the measurement of Ca^{2+} efflux rates (Fig. 8*C*). Addition of ruthe-

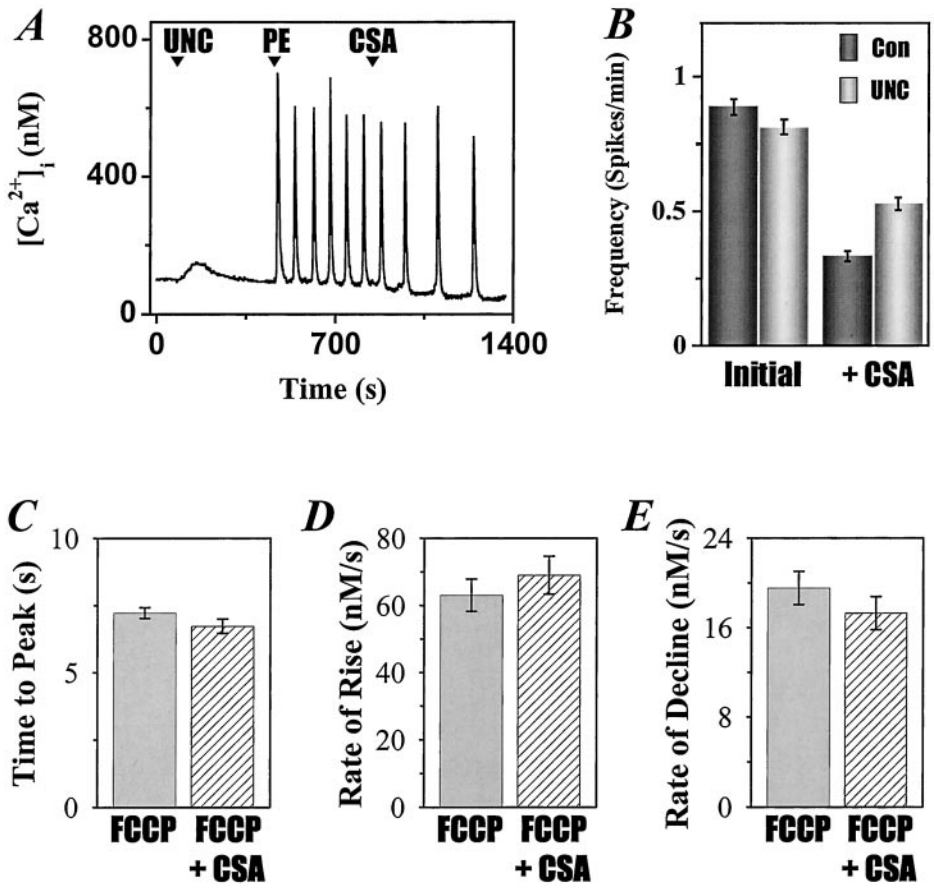

FIG. 9. **Effect of cyclosporin A on the frequency and kinetics of IP_3-dependent $[Ca^{2+}]_i$ oscillations in the absence of mitochondrial Ca^{2+} uptake.** Fura-2/AM-loaded hepatocytes were incubated in KR-HEPES buffer supplemented with glutamate and pyruvate 30 min prior to data acquisition. *A* shows a typical single-cell IP_3-dependent $[Ca^{2+}]_i$ response after inhibiting mitochondrial function. The additions are mitochondrial inhibitors (*UNC*; 5 μM FCCP, 5 μM rotenone, and 5 μg/ml oligomycin), phenylephrine (*PE*; 1.0 μM), and cyclosporin A (*CSA*; 5 μM). *B*, the frequency of PE-induced $[Ca^{2+}]_i$ oscillations was calculated before and after CSA addition in the absence of mitochondrial inhibitors (*Con*). In parallel cultures, hepatocytes were pretreated 5 min with mitochondrial inhibitors (*UNC*) prior to PE stimulation (see *A* for experimental protocol). The data are the means ± S.E. (n = 150–175 cells, four cell preparations) from parallel runs using hepatocytes from the same primary culture. Mitochondrial toxins did not significantly affect the initial frequency of PE-induced $[Ca^{2+}]_i$ spikes (*left*). However, mitochondrial inhibitors significantly reduced the effects of CSA ($p <$ 0.001, right). *C–E*, the effects of CSA on the kinetic properties of PE-induced $[Ca^{2+}]_i$ oscillations in the absence of mitochondrial Ca^{2+} uptake. Data were collected as described in Fig. 2. In the presence of mitochondrial inhibitors (*FCCP + CSA*), CSA did not significantly affect the shape or kinetics of the $[Ca^{2+}]_i$ spike. The data are the means ± S.E. (n = 54 cells, four hepatocyte preparations).

nium red prior to the Ca^{2+} pulse completely blocked all Ca^{2+} uptake (not shown). CSA dramatically suppressed the rate of Ca^{2+} egress ($p < 0.05$; Fig. 8, *C* and *D*), which could account for the large increase in mitochondrial Ca^{2+} content measured in the intact hepatocytes (Fig. 7, *B* and *C*). As expected, FK-506 did not affect mitochondrial Ca^{2+} fluxes (Fig. 8), consistent with intact cell data and the absence of FKBP immunophilins in the mitochondrial matrix (2). Taken together, these results suggest that the higher $\Delta\Psi_m$ in the presence of CSA can increase the driving force for mitochondrial Ca^{2+} uptake. Moreover, transient mitochondrial PTP openings may also function as a route for Ca^{2+} efflux, and CSA appears to inhibit this mitochondrial Ca^{2+} release pathway, as well as enhancing Ca^{2+} uptake by increasing $\Delta\Psi_m$.

Effect of CSA on IP_3-dependent Ca^{2+} Signaling in the Absence of Mitochondrial Ca^{2+} Transport—CSA-dependent stimulation of either Tg-sensitive Ca^{2+} pumps or mitochondrial Ca^{2+} uptake could interfere with local positive Ca^{2+} feedback on the IP_3R. To evaluate the role of the mitochondria in this process, we compared the effects of CSA on IP_3-dependent $[Ca^{2+}]_i$ signals in the presence and absence of mitochondrial inhibitors (*i.e.* FCCP, rotenone, oligomycin; UNC) in intact hepatocytes. As shown previously, $\Delta\Psi_m$ depolarization results in a transient increase in $[Ca^{2+}]_i$ as matrix Ca^{2+} is released (Fig. 9*A*). Under these conditions, cellular ATP does not appear to be limiting for $[Ca^{2+}]_i$ homeostatic mechanisms, because both basal and inter-spike $[Ca^{2+}]_i$ levels remained stable after the initial FCCP-induced $[Ca^{2+}]_i$ response. Importantly, the mitochondrial inhibitors did not prevent IP_3-dependent $[Ca^{2+}]_i$ oscillations (Fig. 9*A*); stimulation with submaximal PE concentrations resulted in repetitive baseline-separated $[Ca^{2+}]_i$ oscillations in 70–80% of the cells, which was not significantly different from control. Moreover, the magnitude of the $[Ca^{2+}]_i$ spike remained the same, $[Ca^{2+}]_i$ peak height was 466 ± 43 nM and 497 ± 26 nM in the absence and presence of mitochondrial toxins, respectively (mean ± S.E.; n = 100–125 cells, nine cell preparations). In the presence of mitochondrial inhibitors, the inhibitory effects of CSA on PE-induced $[Ca^{2+}]_i$ responses was significantly reduced (Fig. 9*B*, *+CSA*). CSA inhibited the frequency of PE-induced $[Ca^{2+}]_i$ oscillations by 62 ± 2% under physiological conditions, but by only 38 ± 2% after blocking mitochondrial Ca^{2+} uptake ($p < 0.001$). Thus, blocking mitochondrial Ca^{2+} uptake reduced the effects of CSA on both IP_3-dependent $[Ca^{2+}]_i$ oscillations in intact cells (Fig. 9*B*) and IP_3-induced Ca^{2+} release in permeabilized hepatocytes (Fig. 6*B*), indicating that mitochondria contribute to the decrease in IP_3R sensitivity.

The rates of rise and fall of individual $[Ca^{2+}]_i$ spikes were significantly increased in the presence of mitochondrial inhibitors ($p < 0.001$; compare Fig. 2, *D–E*, with Fig. 9, *D–E*). However, CSA did not significantly affect the kinetics of the $[Ca^{2+}]_i$ spikes under these conditions (Fig. 9, *C–E*). Thus, the disruption of mitochondrial Ca^{2+} transport eliminated the effects of CSA on the shape of the $[Ca^{2+}]_i$ spike. Half-peak width was 10.6 ± 0.4 and 11.7 ± 0.5 s before and after CSA, respectively ($p > 0.05$). These data suggest that the CSA-mediated decrease in the declining phase of the $[Ca^{2+}]_i$ spike, observed in the absence of mitochondrial inhibitors (Fig. 2*E*), could be explained by an increase in total mitochondrial Ca^{2+} content (Fig. 7*B*) coupled with slower mitochondrial Ca^{2+} egress (Fig. 8*D*).

DISCUSSION

Regulation of Ca^{2+} Transport Mechanisms—The ubiquitous tissue expression, broad subcellular distribution, and multiple protein targets situate the cyclophilin family at a critical juncture to regulate a diverse array of cellular activities (1–3, 5).

Our study has identified two distinct effects of CSA on Ca^{2+} transport pathways in hepatocytes: Tg-sensitive Ca^{2+} pumps and mitochondrial Ca^{2+} uptake and retention. MeVal-CS has similar effects on Ca^{2+} transport mechanisms, indicating that calcineurin is probably not involved. Thus, it would appear that specific cyclophilin isozymes directly regulate these cellular Ca^{2+} transport mechanisms.

In intact hepatocytes, CSA or MeVal-CS stimulated a Tg-sensitive decrease in baseline $[Ca^{2+}]_i$ under resting conditions or during agonist stimulation (Figs. 1–4). This effect on free Ca^{2+} levels could be fully reconstituted in a permeabilized cell system, pointing to an ER-associated cyclophilin as a possible mediator. Several mechanisms could contribute to lower $[Ca^{2+}]_{ex}$ in permeabilized hepatocytes: (*a*) decreased Ca^{2+} leak from internal stores (*b*) increased luminal Ca^{2+}-buffering capacity and/or (*c*) a change in the kinetics properties of the Ca^{2+} pumps. Because CSA does not affect the size of the ionomycin-sensitive Ca^{2+} pool (see text) nor the passive Ca^{2+} leak rate from internal stores (Fig. 5*B*), the first two options do not appear to be major contributors. However, we cannot rule out the loss of cytosolic factors or partial disruption of ER integrity during permeabilization affecting our results. Nevertheless, the simplest explanation is a change in the kinetic properties of the Ca^{2+} pump; an enhanced rate of Ca^{2+} uptake and lower final set point for $[Ca^{2+}]_{ex}$ suggest an increased affinity for Ca^{2+}.

Previous studies have identified members of the cyclophilin family as calreticulin binding proteins (21). In addition to its role as a Ca^{2+} storage protein, calreticulin is also a lectin-like molecular chaperone and participates in the correct folding of newly synthesized glycoproteins (53). Recently, it has been proposed that the chaperon domain of calreticulin might also specifically interact with the mature form of SERCA 2b to modulate IP_3-mediated Ca^{2+} release in *Xenopus* oocytes (54, 55). SERCA 2b is the only isoform expressed in hepatocytes (56) and differs from other SERCA sub-types, containing an additional transmembrane domain that localizes a putative *N*-glycosylation site in the C-terminal to the ER lumen (53). In oocytes, overexpression of calreticulin inhibits the repetitive $[Ca^{2+}]_i$ spikes induced by IP_3 microinjection, apparently by modulating the functional conformation and, thus, Ca^{2+} transport activity of SERCA 2b (54, 55). In this model, dissociation of calreticulin from SERCA 2b restores full enzymatic activity, whereas calreticulin binding reduces Ca^{2+} transport. It is an intriguing possibility that the CSA·cyclophilin complex may directly inhibit calreticulin binding to the Ca^{2+} pump. Alternatively, calreticulin and cyclophilin may form a complex with SERCA 2b, which is disrupted by CSA, a mechanism similar to displacing CyP-D from the mitochondrial PTP (6–8).

CSA is known to inhibit the PTP in isolated mitochondria and suppresses necrotic cell death associated with mitochondrial Ca^{2+} overload in a variety of cells types (6, 12, 13). The CSA-sensitive mitochondrial target is presumably CyP-D; CSA binding disassociates CyP-D from the PTP complex (7, 8) decreasing the open probability of the channel. Classic mitochondrial studies have put forward the concept that PTP opening has irreversible deleterious effects on mitochondrial function. This includes mitochondrial depolarization, release of matrix ions, and the loss mitochondrial metabolites into the cytosol (6). However, more recent evidence suggests that the PTP operates in two distinct conducting states, high conductance involved in the irreversible opening of the pore, and a low conductance mode, more selective to protons and Ca^{2+} (9, 10). In hepatocytes, CSA promoted a stable increase in $\Delta\Psi_m$ (Fig. 7*D*) consistent with the presence of a constitutively active but low conducting state of the PTP that partially dissipates the mitochondrial electrochemical gradient. CSA has also been shown to increase basal $\Delta\Psi_m$ in several other cell types using similar fluorescence imaging techniques (50, 51). Moreover, a spontaneous and transient CSA-sensitive increase in membrane permeability has been reported in single isolated cardiac mitochondria and mitochondria in intact hepatocytes (57, 58). Taken together, these data strongly suggest that CSA-sensitive "pores" or channels undergo cyclical opening and closing to contribute to the basal proton leak rate across the mitochondrial inner membrane.

CSA enhanced mitochondrial Ca^{2+} uptake in both permeabilized and intact hepatocytes while inhibiting Ca^{2+} egress (Figs. 7 and 8). Ca^{2+} transport across the mitochondrial inner membrane is regulated by components of the mitochondrial PMF. The large negative $\Delta\Psi_m$ drives mitochondrial Ca^{2+} uptake through the Ca^{2+} uniporter, whereas both $\Delta\Psi_m$ and the mitochondrial proton gradient can contribute to Ca^{2+} efflux (59). In isolated rat mitochondria, the initial rate of Ca^{2+} uptake increases in proportion to the magnitude of $\Delta\Psi_m$ (52). Thus, the CSA-induced rise in $\Delta\Psi_m$ is the most likely parameter mediating the enhanced rate of mitochondrial Ca^{2+} uptake. In liver, mitochondrial Ca^{2+} efflux is predominately mediated by a Na^+-independent mechanism, presumably H^+/Ca^{2+} exchange, because the Na^+/Ca^{2+} exchanger is suppressed by physiological concentrations of Mg^{2+} in this tissue (59). Both mitochondrial Ca^{2+} efflux mechanisms have been proposed to be electrogenic (60, 61) and thus, Ca^{2+} egress should be stimulated by a rise in $\Delta\Psi_m$ and not suppressed as we observed in this investigation (Fig. 8). Thus, our data suggests two possible alternatives: (*a*) the low conducting mitochondrial PTP is the major Ca^{2+} efflux pathway in hepatocytes or (*b*) the CSA·cyclophilin complex directly inhibits mitochondrial Ca^{2+} efflux pathways.

Effect of CSA on IP_3-dependent $[Ca^{2+}]_i$ Spikes—CSA and MeVal-CS both inhibited the frequency of PE-induced $[Ca^{2+}]_i$ oscillations in a concentration-dependent manner (Fig. 1). In the case of CSA, we show a small, but reproducible, decrease in IP_3 sensitivity in permeabilized hepatocytes (Fig. 6). The rightward shift in the IP_3 concentration response curve was sensitive to inhibitors that eliminated mitochondrial Ca^{2+} uptake (Fig. 6*B*). Moreover, the same inhibitor mixture decreased the effects of CSA on IP_3-dependent Ca^{2+} signals in intact hepatocytes (Fig. 9*B*), indicating that Ca^{2+} uptake by the mitochondria plays a role in shifting IP_3R sensitivity both *in vitro* and *in situ*. We have previously reported that the close association between ER Ca^{2+} release channels and mitochondrial Ca^{2+} uptake sites allows the mitochondria to influence IP_3R excitability by suppressing the local Ca^{2+} gradients surrounding the mouth of the channel (32). The observation that CSA manifests a profound effect on the rate of mitochondrial Ca^{2+} uptake in both permeabilized and intact hepatocytes (Figs. 7 and 8) is consistent with the modulation of IP_3R function through such local Ca^{2+} gradients.

The mitochondria are not the sole participants in this complex mechanism; elimination of mitochondrial Ca^{2+} uptake did not completely reverse the effects of CSA (Figs. 6*B* and 9*B*). Although we cannot absolutely exclude a direct effect of CSA on IP_3R function, the simplest explanation is that the Tg-sensitive Ca^{2+} pumps, together with mitochondria, act synergistically to reset the threshold for initiating a $[Ca^{2+}]_i$ spike. Because Ca^{2+} is involved in both the activation and inactivation of the IP_3R (22–24), Ca^{2+} transport mechanisms would be excepted to influence IP_3R function. Indeed, both SERCA activity and mitochondrial Ca^{2+} uptake have been shown to exert a negative influence on oscillatory $[Ca^{2+}]_i$ signals by suppressing Ca^{2+} spike initiation (32, 62, 63), which is consistent with our interpretation.

CSA prolonged the decay phase of the $[Ca^{2+}]_i$ spike (Fig. 2*E*). We hypothesized that this may reflect slow Ca^{2+} release from the mitochondria, because CSA enhances matrix Ca^{2+} accumulation and retention during agonist stimulation (Figs. 7 and 8). To test for a mitochondrial origin, we inhibited matrix Ca^{2+} transport in intact hepatocytes by depolarizing $\Delta\Psi_m$ with mitochondrial inhibitors prior to agonist stimulation. Depolarizing the mitochondria significantly increased both the rising and falling phases of the $[Ca^{2+}]_i$ spike (compare Figs. 2 and 9). We have previously shown that blocking mitochondrial Ca^{2+} uptake increases the efficacy of submaximal IP_3 to release Ca^{2+} from internal stores (32), which could account for the stimulation of the rising phase of the $[Ca^{2+}]_i$ spike. Moreover, the faster rate of decline is presumably due to the absence of mitochondrial Ca^{2+} being released back to the cytosol. Although some ATP depletion occurs over the time course of these experiments (33), it does not appear to impair $[Ca^{2+}]_i$ homeostasis (Fig. 9*A*). Indeed, the decay rate of the $[Ca^{2+}]_i$ spike increased, not decreased as would be expected if ATP-dependent Ca^{2+} transport was inhibited. Consequently, the effects of mitochondrial toxins on the kinetic properties of the $[Ca^{2+}]_i$ spike appear to be specific to blocking mitochondrial Ca^{2+} transport and not due to a drop in cellular ATP levels.

Importantly, the effects of CSA on the kinetic properties of the $[Ca^{2+}]_i$ spike were eliminated in the presence of mitochondrial inhibitors (Fig. 9). Under physiological conditions, CSA presumably prolongs the $[Ca^{2+}]_i$ transient by increasing mitochondrial Ca^{2+} accumulation during the rising phase of the $[Ca^{2+}]_i$ spike, coupled with a dramatic reduction in mitochondrial Ca^{2+} egress. By contrast, the CSA-induced increase in the rate of rise of the $[Ca^{2+}]_i$ spike (Fig. 2*D*) is probably not due to its action on mitochondria, because inhibition of mitochondrial Ca^{2+} uptake with uncoupler also enhanced the rate of $[Ca^{2+}]_i$ rise (Fig. 9*D*). The effect of CSA on the rate of $[Ca^{2+}]_i$ increase could be explained by its effect on the SERCA pump, either by increasing the pool of ER Ca^{2+} for release, or by increasing the proportion of IP_3Rs in the basal state and available to participate in the Ca^{2+} release process.

Finally, the inhibition of agonist-induced $[Ca^{2+}]_i$ responses was not limited to the cyclophilin family. Preliminary experiments revealed that FK-506, ascomycin, and rapamycin have similar effects on the frequency on hepatic Ca^{2+} signals, although at a reduced efficacy compared with CSA. The relationship between the FKBP family of proteins and IP_3-dependent $[Ca^{2+}]_i$ responses is still under investigation. To date, none of the FKBP binding drugs have been shown to effect plasma membrane Ca^{2+} fluxes, whereas each drug potently stimulates a Tg-sensitive decrease in basal $[Ca^{2+}]_i$. Moreover, these drugs do not modify mitochondrial Ca^{2+} transport in permeabilized cell suspensions (Fig. 7), which is consistent with a lack of FKBPs in the mitochondrial matrix (2). Thus, it would appear that cyclophilins and FKBPs can both regulate specific Ca^{2+} transport pathways, thereby influencing IP_3-dependent $[Ca^{2+}]_i$ responses.

Mitochondria and Ca^{2+} Signaling—Mitochondria are well known participants in the regulation of $[Ca^{2+}]_i$ homeostasis, capable of modulating cytosolic Ca^{2+} signals (9, 63–67) and exerting local control over IP_3R excitability (32). In many cells, the ER envelops the mitochondria placing the mitochondrial Ca^{2+} uptake sites in juxtaposition to the IP_3Rs (68) or to the RyRs (69). Thus, mitochondria have privileged access to the highly localized Ca^{2+} gradients generated during ligand-induced ER Ca^{2+} mobilization (28, 67, 70, 71). This strategic location facilitates the activation of mitochondrial Ca^{2+} uptake and, thus, Ca^{2+}-dependent regulation of metabolic processes in the mitochondrial matrix (33, 36). Moreover, in some cell types, these local Ca^{2+} gradients may also serve as a trigging mechanism to open the mitochondrial PTP, resulting in mitochondrial calcium-induced calcium-release and amplification of IP_3-dependent $[Ca^{2+}]_i$ spikes (9).

Our data are clearly consistent with the mitochondria playing an important role in setting the frequency and modulating the kinetic properties of IP_3-dependent $[Ca^{2+}]_i$ oscillations in hepatocytes. However, it is worth emphasizing several points regarding the role of the mitochondria in IP_3-dependent $[Ca^{2+}]_i$ signaling. First, functional mitochondria are not essential components required to generate oscillatory Ca^{2+} signals in hepatocytes (Fig. 9), consistent with our previous suggestion that only IP_3 and Ca^{2+} are needed to produce periodic opening and closing of the IP_3R (31). Second, in contrast to previous reports, blocking mitochondrial Ca^{2+} uptake does not affect the magnitude of the $[Ca^{2+}]_i$ spike (reviewed in Ref. 14), indicating that other Ca^{2+} transport mechanisms or cellular Ca^{2+} buffers regulate peak height. Nevertheless, mitochondrial Ca^{2+} uptake can alter the kinetics properties of the $[Ca^{2+}]_i$ spike (Fig. 9) and modulate the propagation rate of intracellular Ca^{2+} waves (32). Finally, our data are not consistent with localized Ca^{2+} gradients triggering the opening of the mitochondrial PTP. In hepatocytes, total mitochondrial PMF increases during IP_3-dependent Ca^{2+} mobilization (33, 36) inconsistent with the opening of a large pore in the inner mitochondrial membrane. Perhaps, the sluggish rate of mitochondrial Ca^{2+} uptake, time-to-peak ~14 s (33), is insufficient to "trigger" the PTP into the low conductance mode required for $\Delta\Psi_m$ depolarization and subsequent rapid matrix Ca^{2+} release. Nevertheless, the mitochondrial CSA-sensitive Ca^{2+} release pathway should still have profound effects on the activation of cytosolic Ca^{2+}-sensitive targets, such as CaM kinase II (72), by controlling the duration of the $[Ca^{2+}]_i$ spike.

In summary, the properties of hepatic mitochondria devise a potentially complex feedback mechanism to modulate oscillatory Ca^{2+} signals. The close association between ER and mitochondrial membranes (68) ensures efficient transfer of Ca^{2+} between the organelles during IP_3-dependent Ca^{2+} mobilization. The initial $[Ca^{2+}]_i$ spike would activate Ca^{2+}-dependent metabolic pathways in the mitochondrial matrix stimulating the respiratory chain (28, 33, 36) and increasing the driving force for mitochondrial Ca^{2+} uptake which, in turn, suppresses the initiation of subsequent $[Ca^{2+}]_i$ spikes. Thus, the mitochondria may set the upper limit for the frequency of IP_3-dependent $[Ca^{2+}]_i$ oscillations. A feedback mechanism, including the mitochondria balances the need for stimulating ATP production without exposing the mitochondria or the cytosol to excessive $[Ca^{2+}]_i$ signals, beyond what is required to maximally stimulate metabolism.

Acknowledgments—We thank Dr. Anthony J. Morgan for the decisive interaction and discussion with the permeabilized hepatocytes experiments and Drs. Basal Hantash, Sandip Patel, and John Reeves for helpful discussion during the execution of this work.

REFERENCES

1. Galat, A. (1993) *Eur. J. Biochem.* **216,** 689–707
2. Fruman, D. A., Burakoff, S. J., and Bierer, B. E. (1994) *FASEB J.* **8,** 391–400
3. Marks, A. R. (1996) *Physiol. Rev.* **76,** 631–649
4. Liu, J., Farmer, J. D., Jr., Lane, W. S., Friedman, J., Weissman, I., and Schreiber, S. L. (1991) *Cell* **66,** 807–815
5. Snyder, S. H., Sabatini, D. M., Lai, M. M., Steiner, J. P., Hamilton, G. S., and Suzdak, P. D. (1998) *Trends Pharmacol. Sci.* **19,** 21–26
6. Zoratti, M., and Szabo, I. (1995) *Biochim. Biophys. Acta* **1241,** 139–176
7. Crompton, M., Virji, S., and Ward, J. M. (1998) *Eur. J. Biochem.* **258,** 729–735
8. Woodfield, K., Ruck, A., Brdiczka, D., and Halestrap, A. P. (1998) *Biochem. J.* **336,** 287–290
9. Ichas, F., Jouaville, L. S., and Mazat, J. P. (1997) *Cell* **89,** 1145–1153
10. Ichas, F., and Mazat, J. P. (1998) *Biochim. Biophys Acta* **1366,** 33–50
11. Kroemer, G., Dallaporta, B., and Resche-Rigon, M. (1998) *Annu. Rev. Physiol.* **60,** 619–642
12. Lemasters, J. J., Nieminen, A. L., Qian, T., Trost, L. C., Elmore, S. P., Nishimura, Y., Crowe, R. A., Cascio, W. E., Bradham, C. A., Brenner, D. A.,

and Herman, B. (1998) *Biochim. Biophys. Acta* **1366,** 177–196
13. Crompton, M. (1999) *Biochem. J.* **341,** 233–249
14. Duchen, M. R. (1999) *J. Physiol. (Lond.)* **516,** 1–17
15. Smaili, S. S., Hsu, Y.-H., Youle, R. J., and Russell, J. T. (2000) *J. Bioenerg. Biomembr.* **32,** 35–46
16. Brillantes, A. B., Ondrias, K., Scott, A., Kobrinsky, E., Ondriasova, E., Moschella, M. C., Jayaraman, T., Landers, M., Ehrlich, B. E., and Marks, A. R. (1994) *Cell* **77,** 513–523
17. Cameron, A. M., Steiner, J. P., Roskams, A. J., Ali, S. M., Ronnett, G. V., and Snyder, S. H. (1995) *Cell* **83,** 463–472
18. Cameron, A. M., Steiner, J. P., Sabatini, D. M., Kaplin, A. I., Walensky, L. D., and Snyder, S. H. (1995) *Proc. Natl. Acad. Sci. U. S. A.* **92,** 1784–1788
19. Cameron, A. M., Nucifora, F. C., Jr., Fung, E. T., Livingston, D. J., Aldape, R. A., Ross, C. A., and Snyder, S. H. (1997) *J. Biol. Chem.* **272,** 27582–27588
20. Arber, S., Krause, K. H., and Caroni, P. (1992) *J. Cell Biol.* **116,** 113–125
21. Reddy, P. A., and Atreya, C. D. (1999) *Int. J. Biol. Macromol.* **25,** 345–351
22. Berridge, M. J. (1993) *Nature* **361,** 315–325
23. Berridge, M. J., Bootman, M. D., and Lipp, P. (1998) *Nature* **395,** 645–648
24. Thomas, A. P., Bird, G. S., Hajnóczky, G., Robb-Gaspers, L. D., and Putney, J. W., Jr. (1996) *FASEB J.* **10,** 1505–1517
25. Li, W., Llopis, J., Whitney, M., Zlokarnik, G., and Tsien, R. Y. (1998) *Nature* **392,** 936–941
26. Gu, X., and Spitzer, N. C. (1995) *Nature* **375,** 784–787
27. Dolmetsch, R. E., Xu, K., and Lewis, R. S. (1998) *Nature* **392,** 933–936
28. Hajnóczky, G., Robb-Gaspers, L. D., Seitz, M. B., and Thomas, A. P. (1995) *Cell* **82,** 415–424
29. Patel, S., Joseph, S. K., and Thomas, A. P. (1999) *Cell Calcium* **25,** 247–264
30. Putney, J. W., Jr., and Bird, G. S. (1993) *Endocr. Rev.* **14,** 610–631
31. Hajnoczky, G., and Thomas, A. P. (1997) *EMBO J.* **16,** 3533–3543
32. Hajnoczky, G., Hager, R., and Thomas, A. P. (1999) *J. Biol. Chem.* **274,** 14157–14162
33. Robb-Gaspers, L. D., Burnett, P., Rutter, G. A., Denton, R. M., Rizzuto, R., and Thomas, A. P. (1998) *EMBO J.* **17,** 4987–5000
34. Rooney, T. A., Sass, E. J., and Thomas, A. P. (1989) *J. Biol. Chem.* **264,** 17131–17141
35. Morgan, A. J., and Thomas, A. P. (1999) *Methods Mol. Biol.* **114,** 93–123
36. Robb-Gaspers, L. D., Rutter, G. A., Burnett, P., Hajnoczky, G., Denton, R. M., and Thomas, A. P. (1998) *Biochim. Biophys. Acta* **1366,** 17–32
37. Gregory, R. B., and Berry, M. N. (1991) *Biochim. Biophys. Acta* **1098,** 61–67
38. Thomas, A. P. (1988) *J. Biol. Chem.* **263,** 2704–2711
39. Nicolli, A., Basso, E., Petronilli, V., Wenger, R. M., and Bernardi, P. (1996) *J. Biol. Chem.* **271,** 2185–2192
40. Liu, J., Albers, M. W., Wandless, T. J., Luan, S., Alberg, D. G., Belshaw, P. J., Cohen, P., MacKintosh, C., Klee, C. B., and Schreiber, S. L. (1992) *Biochemistry* **31,** 3896–3901
41. Fliri, H., Baumann, G., Enz, A., Kallen, J., Luyten, M., Mikol, V., Movva, R., Quesniaux, V., Schreier, M., Walkinshaw, M., Wenger, R., Zenke, G., and Zurini, M. (1993) Ann. N. Y. Acad. Sci. **696,** 47–53
42. Schreier, M. H., Baumann, G., and Zenke, G. (1993) *Transplant Proc.* **25,** 502–507
43. Nathanson, M. H. (1994) *Gastroenterology* **106,** 1349–1364
44. Kroner, H. (1986) *Arch. Biochem. Biophys* **251,** 525–535
45. Kroner, H. (1986) *Biol. Chem. Hoppe-Seyler* **367,** 483–493
46. Marshall, I. C., and Taylor, C. W. (1993) *J. Biol. Chem.* **268,** 13214–13220
47. Nicchitta, C. V., Kamoun, M., and Williamson, J. R. (1985) *J. Biol. Chem.* **260,** 13613–13618
48. Altschuld, R. A., Hohl, C. M., Castillo, L. C., Garleb, A. A., Starling, R. C., and Brierley, G. P. (1992) *Am. J. Physiol.* **262,** H1699–H1704
49. Hoek, J. B., Farber, J. L., Thomas, A. P., and Wang, X. (1995) *Biochim. Biophys. Acta* **1271,** 93–102
50. Fall, C. P., and Bennett, J. P., Jr. (1999) *Biochim. Biophys. Acta* **1410,** 77–84
51. Smaili, S. S., and Russell, J. T. (1999) *Cell Calcium* **26,** 121–130
52. Wingrove, D. E., Amatruda, J. M., and Gunter, T. E. (1984) *J. Biol. Chem.* **259,** 9390–9394
53. Michalak, M., Corbett, E. F., Mesaeli, N., Nakamura, K., and Opas, M. (1999) *Biochem. J.* **344,** 281–292
54. John, L. M., Lechleiter, J. D., and Camacho, P. (1998) *J. Cell Biol.* **142,** 963–973
55. Camacho, P., and Lechleiter, J. D. (1995) *Cell* **82,** 765–771
56. Lievremont, J. P., Hill, A. M., Hilly, M., and Mauger, J. P. (1994) *Biochem. J.* **300,** 419–427
57. Huser, J., Rechenmacher, C. E., and Blatter, L. A. (1998) *Biophys J.* **74,** 2129–2137
58. Petronilli, V., Miotto, G., Canton, M., Brini, M., Colonna, R., Bernardi, P., and Di Lisa, F. (1999) *Biophys J.* **76,** 725–734
59. Gunter, T. E., and Pfeiffer, D. R. (1990) *Am. J. Physiol.* **258,** C755–C786
60. Gunter, K. K., Zuscik, M. J., and Gunter, T. E. (1991) *J. Biol. Chem.* **266,** 21640–21648
61. Jung, D. W., Baysal, K., and Brierley, G. P. (1995) *J. Biol. Chem.* **270,** 672–678
62. Morgan, A. J., and Jacob, R. (1998) *J. Physiol. (Lond.)* **513,** 83–101
63. Jouaville, L. S., Ichas, F., Holmuhamedov, E. L., Camacho, P., and Lechleiter, J. D. (1995) *Nature* **377,** 438–441
64. Hoth, M., Fanger, C. M., and Lewis, R. S. (1997) *J. Cell Biol.* **137,** 633–648
65. Babcock, D. F., Herrington, J., Goodwin, P. C., Park, Y. B., and Hille, B. (1997) *J. Cell Biol.* **136,** 833–844
66. Budd, S. L., and Nicholls, D. G. (1996) *J. Neurochem.* **67,** 2282–2291
67. Simpson, P. B., Mehotra, S., Lange, G. D., and Russell, J. T. (1997) *J. Biol. Chem.* **272,** 22654–22661
68. Rizzuto, R., Pinton, P., Carrington, W., Fay, F. S., Fogarty, K. E., Lifshitz, L. M., Tuft, R. A., and Pozzan, T. (1998) *Science* **280,** 1763–1766
69. Ramesh, V., Sharma, V. K., Sheu, S. S., and Franzini-Armstrong, C. (1998) *Ann. N. Y. Acad. Sci.* **853,** 341–344
70. Rizzuto, R., Brini, M., Murgia, M., and Pozzan, T. (1993) *Science* **262,** 744–747
71. Simpson, P. B., and Russell, J. T. (1996) *J. Biol. Chem.* **271,** 33493–33501
72. De Koninck, P., and Schulman, H. (1998) *Science* **279,** 227–230

Cyclosporin A Inhibits Inositol 1,4,5-Trisphosphate-dependent Ca^{2+} Signals by Enhancing Ca^{2+} Uptake into the Endoplasmic Reticulum and Mitochondria

Soraya S. Smaili, Kerri Anne Stellato, Paul Burnett, Andrew P. Thomas and Lawrence D. Gaspers

J. Biol. Chem. 2001, 276:23329-23340.
doi: 10.1074/jbc.M100989200 originally published online April 25, 2001
